

1
2
3
4
5
6
7
8
9
10
11
12
13
14
15
16
17
18
19
20

The most widespread phage in animals:

Genomics and taxonomic classification of Phage WO

Sarah R. Bordenstein*^{1,2} and Seth R. Bordenstein^{1,2,3,4}

¹ Department of Biological Sciences, Vanderbilt University, Nashville, Tennessee, USA

² Vanderbilt Microbiome Innovation Center, Vanderbilt University, Nashville, Tennessee, USA

³ Department of Pathology, Microbiology and Immunology, Vanderbilt University, Nashville, Tennessee, USA

⁴ Vanderbilt Institute of Infection, Immunology, and Inflammation, Vanderbilt University, Nashville, Tennessee, USA

* Corresponding Author:

Sarah R. Bordenstein, Department of Biological Sciences, Vanderbilt University, Nashville, Tennessee, USA, 615-343-2647, sarah.bordenstein@vanderbilt.edu

21 **Abstract**

22 *Wolbachia* are the most common obligate, intracellular bacteria in animals. They exist worldwide
23 in arthropod and nematode hosts in which they commonly act as reproductive parasites or
24 mutualists, respectively. Bacteriophage WO, the largest of *Wolbachia*'s mobile elements, includes
25 reproductive parasitism genes, serves as a hotspot for genetic divergence and genomic
26 rearrangement of the bacterial chromosome, and uniquely encodes a Eukaryotic Association
27 Module with eukaryotic-like genes and an ensemble of putative host interaction genes. Despite
28 WO's relevance to genome evolution, selfish genetics, and symbiotic applications, relatively little
29 is known about its origin, host range, diversification, and taxonomic classification. Here we
30 analyze the most comprehensive set of 150 *Wolbachia* and phage WO assemblies to provide a
31 framework for discretely organizing and naming integrated phage WO genomes. We demonstrate
32 that WO is principally in arthropod *Wolbachia* with relatives in diverse endosymbionts and
33 metagenomes, organized into four variants related by gene synteny, often oriented opposite the
34 origin of replication in the *Wolbachia* chromosome, and the large serine recombinase is an ideal
35 typing tool to assign taxonomic classification of the four variants. We identify a novel, putative
36 lytic cassette and WO's association with a conserved eleven gene island, termed Undecim Cluster,
37 that is enriched with virulence-like genes. Finally, we evaluate WO-like Islands in the *Wolbachia*
38 genome and discuss a new model in which Octomom, a notable WO-like Island, arose from a split
39 with WO. Together, these findings establish the first comprehensive Linnaean taxonomic
40 classification of endosymbiont phages that includes distinguishable genera of phage WO, a family
41 of non-*Wolbachia* phages from aquatic environments, and an order that captures the collective
42 relatedness of these viruses.

43

44 **Introduction**

45 Intracellular, endosymbiotic bacteria comprise some of the most intimate and enduring host-
46 microbe interactions. While reductive evolutionary forces are often presumed to lead to
47 streamlined, tiny genomes, many endosymbionts that host switch contain notable levels of active
48 or relic mobile DNA [1]. An exemplar is the genus *Wolbachia* which harbor transposons [2],
49 temperate phages [3, 4], and putative plasmids [5, 6]. *Wolbachia* are members of the
50 Anaplasmataceae family [7] that also includes the intracellular genera *Anaplasma*, *Ehrlichia*,
51 *Neorickettsia*, *Aegyptianella*, and several newly classified bacteria. *Wolbachia* occur in a vast
52 number of invertebrates spanning some nematodes and roughly half of all arthropod species, thus
53 making them the most widespread endosymbionts in animals [8]; but unlike its sister genera, it
54 does not naturally occur in mammalian hosts [9]. Transmission routes are predominantly vertical
55 through the germline, and horizontal transmission of *Wolbachia* in arthropods is frequent on an
56 evolutionary timescale [10, 11], leading to coinfections and subsequent bacteriophage exchanges
57 in the same host [12-16]. Integrated within the bacterial chromosome, these bacteriophages are hot
58 spots of genetic divergence between *Wolbachia* strains [6, 17-20].

59
60 Many arthropod-associated *Wolbachia* cause various forms of reproductive parasitism including
61 feminization, parthenogenesis, male killing, and cytoplasmic incompatibility (CI). These selfish
62 modifications hijack sex determination, sex ratios, gametogenesis, and/or embryonic viability to
63 enhance the spread of *Wolbachia* through the transmitting matriline [21, 22]. Nematode-associated
64 *Wolbachia*, however, generally lack phage WO and more often act as mutualists within their
65 animal host [23, 24]. Thus, phage WO was originally hypothesized to contribute to these
66 reproductive manipulations in arthropods through horizontal acquisition and differential

67 expression of parasitism genes that are not part of the core *Wolbachia* genome [20, 23, 25-28].
68 Indeed, transgenic expression of two genes from phage WO or WO-like Islands (genomic islands
69 that are associated with and/or derived from phage WO) demonstrated cytoplasmic incompatibility
70 factors *cifA* and *cifB* as the primary cause of *Wolbachia*-induced CI and rescue [29-32]. In addition,
71 transgenic expression of the WO-mediated killing gene *wmk* recapitulates male-specific embryo
72 lethality and is a candidate for male killing [33]. Conversely, lytic activity of phage WO associates
73 with reduced *Wolbachia* densities and CI levels [34].

74
75 First observed in 1978 as “virus-like bodies” within the gonads of *Culex pipiens* mosquitoes [35],
76 phage WO is a temperate phage that exists in a lysogenic state (the integrated form of a phage
77 genome is termed a prophage) until an event triggers particle production and subsequent lysis of
78 the cell [4, 34, 36-38]. Unlike phages of free-living bacteria, however, the phage particles of
79 intracellular *Wolbachia* contend with a two-fold cell challenge of bacterial and eukaryotic-derived
80 membranes surrounding *Wolbachia* as well as the cytoplasmic and/or extracellular environments
81 of the eukaryotic host. These unique challenges encountered by phage WO presumably selected
82 for the evolution of a novel Eukaryotic Association Module (EAM) that comprises up to 60% of
83 its genome with genes that are eukaryotic-like in function and/or origin [39]. The phage WO
84 genome also features one of the longest genes ever identified in a phage and an abundance of
85 ankyrin repeat domain genes [20, 23, 34, 40, 41], though their function has not been clearly
86 elucidated as it has for the Ankyphages of sponge symbionts that aid in the evasion of the
87 eukaryotic immune system [42]. Given the abundance and importance of phage WO in *Wolbachia*
88 and for understanding genomic flux in endosymbioses worldwide, a firm grasp of its biology,

89 including classification, evolution, and functions, will be important for establishing and comparing
90 the rules across systems of endosymbiotic phages.

91

92 Here we survey prophage WO from 150 *Wolbachia* genome assemblies currently available in the
93 NCBI database [43]. We report the patterns of distribution, chromosomal location, and functions
94 of WO, and we propose a Linnaean classification system according to consultation with the
95 International Committee and their guidelines on Taxonomy of Viruses (ICTV) [44, 45] in which
96 there are three distinguishable phage WO genera within a new taxonomic order encompassing
97 prophages of obligate, intracellular bacteria. We show that WO generally occurs in arthropod-
98 associated *Wolbachia*, and prophage insertions are enriched away from the origin of replication in
99 the bacterial chromosome. We fully annotate the EAM boundaries of representative WO genomes
100 and highlight the presence of the CI genes, *cifA* and *cifB*, and a conserved set of eleven genes,
101 defined here as the *Undecim Cluster*. We also establish a new model suggesting Octomom is
102 derived from the EAM of prophage WO, with implications for Octomom-based pathogenicity, and
103 we determine that all intact prophage WO genomes have a putatively novel patatin-based lytic
104 cassette immediately upstream from the tail module. Finally, we report for the first time, to our
105 knowledge, that prophage WO-like variants occur in diverse bacterial endosymbionts as well as
106 metagenomes of putative symbionts from aquatic environments, providing a deeper understanding
107 of WO origins, evolution, and ecology within and between endosymbiotic bacteria.

108

109

110 **Results**

111 **Comprehensive survey of *Wolbachia*'s prophage WO and WO-like**

112 **Islands**

113

114 **Prophage WO elements generally occur in arthropod-associated *Wolbachia***

115 *Wolbachia* occur in many protosome animal species of the superphylum Ecdysozoa, while
116 prophage WO has previously been described as restricted to arthropod-associated strains. Because
117 WO molecular surveys typically use single gene markers [15, 16], we comprehensively explored
118 the NCBI database for prevalence of prophage WO, as determined by presence of one or more
119 core phage WO genes (Fig 1a), throughout all sequenced *Wolbachia* genomes. All *Wolbachia*
120 strains are indicated by a lower-case *w* followed by descriptor of host species, and prophage WO
121 genomes are indicated by a WO prefix followed by the same host descriptor (listed in S1 Table).

122

123 **Fig 1. Prophage WO is modular in structure and associated with all arthropod-infecting *Wolbachia*.** (a) A
124 genomic map of prophage WOMelB from the *D. melanogaster* wMel *Wolbachia* strain highlights phage WO core
125 genes in blue and EAM genes in gray. Genes are illustrated as arrows and direction correlates with forward/reverse
126 strand. The phage WO core consists of recombinase (green), connector/baseplate (royal blue), head (purple),
127 replication and repair (light blue), tail fiber (light pink), tail (salmon), and lysis (brown). The WOMelB EAM encodes
128 *cifA* and *cifB* (cotton candy pink), WO-PC2 containing HTH_XRE transcriptional regulators (lavender), and a
129 conserved set of genes termed the *Undecim Cluster* (navy blue). (b) At least one phage WO core gene (teal) is
130 associated with all sequenced arthropod-*Wolbachia* Supergroups and Supergroup F, which infects both arthropods
131 (blue) and nematodes (purple). The Undecim Cluster (navy blue) is found in the majority of Supergroup A, B, E, and
132 M *Wolbachia* genomes, and CI genes (pink) are encoded by the majority of Supergroup A, B, T, and F genomes.
133 Phage WO elements are absent from all strictly-nematode *Wolbachia* Supergroups. The number of genomes analyzed

134 is listed in parentheses above each Supergroup. Each bar indicates the % of genomes containing each phage WO
135 element. Source data is provided in S1 Table.

136

137 Out of 150 assemblies across nematode and arthropod *Wolbachia*, phage WO occurs in arthropod
138 *Wolbachia* with one exception from the mixed host supergroup of F *Wolbachia* (Fig 1b; S1 Table).

139 All arthropod-associated strains contained evidence of intact or relic phage WO, termed WO-like

140 Islands, and the single instance of WO genes in a nematode occurs in strain *wMhie* from

141 *Madathamugadia hiepei*, a parasite of the insectivorous South African gecko. The *wMhie* genome

142 encodes four genes that are conserved throughout phage WO's transcriptional regulation and

143 replication/repair modules (S2 Table) and are not part of the core *Wolbachia* genome.

144 Interestingly, *wMhie* is a member of Supergroup F that occurs in both arthropods and nematodes.

145 Thus, the presence of phage WO genes in this *Wolbachia* genome supports a horizontal transfer of

146 WO from arthropods to nematodes.

147

148 In addition to core phage WO genes, we characterized the widespread distribution of two phage

149 WO elements across arthropod *Wolbachia*: (i) the cytoplasmic incompatibility factor genes *cifA*

150 and *cifB* and (ii) Undecim Cluster (Fig 1b). Generally located within phage WO's Eukaryotic

151 Association Module (EAM [39]; Fig 1a) or in WO-like Islands (genomic islands that are associated

152 with and/or derived from phage WO), *cifA* and *cifB* occur in Supergroups A, B, F, and T; the latter

153 two are newly reported here. *Wolbachia* strains *wMov* and *wOc* of Supergroup F both encode

154 phylogenetic Type I *cifA* and *cifB* genes, whereas *wChem* of Supergroup T encodes Type II *cifA*

155 and *cifB* genes (S3 Table; See [29, 46, 47] for a discussion of *cif* Types). Likewise, we identified

156 a highly conserved set of eleven phage WO-associated genes, hereby termed the Undecim Cluster

157 (Fig 1a, discussed below), that is distributed across most arthropod Supergroups but notably absent
158 from all nematode *Wolbachia* genomes.

159

160 **Characterizing the prophage WO genome**

161

162 **Prophage WO genomes are comprised of conserved structural modules and a** 163 **Eukaryotic Association Module**

164 Prophage WO genomes adhere to the “modular theory” of phage evolution [18] and thus contain
165 conserved structural gene modules (See discussion in S1 Text) and a Eukaryotic Association
166 Module (EAM) [39]. To date, the EAM is unique to *Wolbachia*’s phage WO and as such is often
167 overlooked by prophage prediction algorithms during the bacterial genome assembly process.
168 Moreover, WO can markedly vary in gene content and synteny, and whether this variation does or
169 does not sort into discrete genomic variants has not been investigated. Thus, we sought to identify
170 conserved and distinguishing genomic features for a comprehensive nomenclature system for the
171 community to classify phage WO major groupings. We mapped and re-annotated prophage WO
172 regions from fully sequenced *Wolbachia* genomes to include the EAM and, more generally,
173 incorporate updated annotations for each module.

174

175 All prophage WO regions were manually curated based on gene content and synteny (Fig 2; S1-
176 S7 Figs) with regards to eight core phage modules (recombinase, replication & repair, head,
177 connector/baseplate, putative tail fiber, tail, putative lysis, and EAM; labeled in Fig 1) and three
178 newly identified and highly conserved gene clusters shown in Fig 2: (i) WO protein cluster 1 (WO-
179 PC1), corresponding to hypothetical proteins WOCauB3_gp2-gp3; (ii) WO protein cluster 2 (WO-

180 PC2), located within the EAM and corresponding to putative HTH_XRE transcriptional regulators,
181 DUF2466 (formerly RadC), and hypothetical proteins WOMeIB_WD0622-WD0626; and (iii) the
182 Undecim Cluster, an eleven-gene region located within the EAM and corresponding to
183 WOMeIB_WD0611-WD0621.

184

185 **Fig 2. Prophage WO variants feature distinguishable module synteny.** Prophage WO variants are organized by
186 genome content and synteny of their structural modules. Sr1WO and sr2WO feature a 5'-core prophage WO region
187 (blue) and a 3'-EAM (gray). Sr3WO features an internal core prophage WO region that is flanked by EAM genes and
188 mobile elements (yellow). Sr4WO is only present in *wFol* and features three genomic regions with multiple prophage
189 segments. WO-like Islands feature small clusters of prophage WO-like genes; they are comprised of singular structural
190 modules and/or subsets of EAM genes. All modules are color coded: green = recombinase; turquoise = WO-PC1; light
191 blue = replication; purple = head; blue = connector/baseplate; light pink = tail fiber; salmon = tail; brown = putative
192 lysis; lavender = WO-PC2; and navy blue = Undecim Cluster. In addition, ankyrins are shown in red; transposable
193 elements are shown in yellow; and *cifA*/*cifB* are shown in cotton candy pink. Dotted lines represent breaks in the
194 assembly; module organization is estimated based on closely related variants. Sr1WO is highlighted in hot pink;
195 sr2WO is highlighted in green; sr3WO is highlighted in purple; sr4WO is highlighted in blue; WO-like Islands are
196 highlighted in gray.

197

198

199 **There are four distinguishable prophage WO variants: sr1WO, sr2WO,**
200 **sr3WO, and sr4WO**

201 While gene synteny within each core module is generally consistent, the arrangement of modules
202 across prophage genomes is variable and does not correlate with the early organization of *orf7*-
203 based WO clades, WO-A and WO-B [16, 48]. To formally update this classification with a more
204 comprehensive classification system, we identified conserved WO loci and modular synteny

205 diagnostic of the four WO arrangement groupings that reflect genus-level ranking. Sequence
206 variation in one gene candidate was consistently associated with similar variation in gene content
207 and synteny: the large serine recombinase [18, 49]. Phage-encoded large serine recombinases
208 facilitate integration of the phage genome into specific attachment sites within the bacterial
209 chromosome as well as control the excision, often with the help of an accessory protein, of the
210 prophage genome during the lytic cycle [50]. A BLASTN analysis of the WO serine recombinase
211 gene confirmed that only those associated with comparable WO module arrangement were full-
212 length reciprocal BLAST hits. Phylogenetic analysis of the recombinase peptide sequence also
213 supported four distinct genus-level clades of prophage WO (common names sr1WO, sr2WO,
214 sr3WO, and sr4WO; nomenclature proposed in [49] and based on the “serine recombinase”) as
215 well as closely-related recombinases in prophage regions of non-*Wolbachia* endosymbionts,
216 including the *Paramecium* endosymbiont *Holospora obtusa* (Fig 3a). The genomic content,
217 organization, and chromosomal integration of each srWO variant are described below.

218

219 **Fig 3. Phylogeny of prophage WO’s large serine recombinase correlates with module synteny and genomic**
220 **integration.** (a) A phylogenetic tree of prophage WO’s recombinase sequence illustrates the utility of this gene as a
221 WO-typing tool to classify prophage WO variants. Four distinct clades correlate with sr1WO-sr4WO genome
222 organization shown in Fig 2. Non-*Wolbachia* sequences represent similar prophages from other bacterial hosts, such
223 as the prophage HOObt1 of *Holospora obtusa*, an endonuclear symbiont of *Paramecium*. The tree was generated by
224 Bayesian analysis of 283 amino acids using the JTT-IG model of evolution. Consensus support values are indicated
225 for each branch. (*) indicates that the prophage regions are highly degraded; while they likely originated from the
226 corresponding prophage group, they are now classified as WO-like Islands (S7 Fig). (b) Prophage WO integration loci
227 are concentrated opposite the origin of replication, *ori*. All *Wolbachia* genomes have been standardized where each
228 dot represents % nucleotide distance calculated by: (nucleotide distance between 5’-WO and *ori* / genome size) * 100.

229 (†) indicates the genome is not closed/circularized; genomic locations are estimated based on alignment of contigs to
230 a reference genome (obtained from authors in [51, 52]).

231

232 *sr1WO*. The proposed genus-level taxonomic name for sr1WO, described below, is Cautellavirus.
233 Most sr1WO recombinases integrate into *Wolbachia*'s magnesium chelatase gene, as we
234 previously reported [39], with portions of the bacterial gene found flanking either side of the
235 prophage region. Two exceptions are in: (i) closely-related wRi and wAna where the sr1WO
236 prophage has since been rearranged in the *Wolbachia* genome (S1 Fig) with a portion of the
237 magnesium chelatase now associated with each prophage fragment (S8a-b Fig); and (ii) wCauB
238 which contains at least two sr1WO prophages, and WOCauB3 has a secondary intergenic
239 attachment site between *sua5* and a hypothetical protein (S8c Fig).

240

241 A key characteristic of sr1WOs is the single domain HTH_XRE transcriptional regulators of WO-
242 PC2 (S1 Fig, lavender) that are located at the 3'-end of the prophage region. Because the genes
243 are fused in most other WO prophages, they are sometimes annotated as pseudogenes (i.e.,
244 wRi_p006660 and wRi_p006630 of WORiC) in the *Wolbachia* genome; however, conservation
245 across multiple variants suggests they are functional. Sr1WOs also lack the methylase/ParB gene
246 that is associated with all other WO prophages. A few genomes (i.e, WORiC, WOAnaC,
247 WOSuziC) harbor *cifA* and *cifB* genes, though the origin of these genes remains inconclusive due
248 to a downstream, highly-pseudogenized sr3WO recombinase (wRi_p006680) and adjacent
249 transposases. Finally, all members of the sr1WO group have a distinct 5'-core-prophage region
250 followed by an ankyrin-rich 3'-EAM (Fig 2 and S1 Fig).

251

252 *sr2WO*. The proposed genus-level taxonomic name for *sr2WO*, described below, is *Vitrivirus*.
253 *sr2WO* prophages genes are also organized as 5'-core-prophage followed by 3'-EAM (Fig 2 and
254 S2 Fig), yet module synteny is quite distinct from *sr1WO*: (i) they lack WO-PC1; (ii) the
255 replication, head, and connector/baseplate modules are reversed; (iii) WO-PC2 is located at the
256 juncture between the core-prophage and EAM regions rather than at the terminal 3'-end of the
257 prophage genome; and (iv) *cifA* and *cifB* genes are absent from assembled genomes thus far. The
258 *sr2WO* recombinase integrates into variable number tandem repeat 105 (VNTR-105) as previously
259 reported [39], a conserved intergenic region used to type closely-related *A-Wolbachia* strains [53].
260 While flanking, disrupted portions of the magnesium chelatase correlate with prophage boundaries
261 of *sr1WO* genomes, disrupted VNTR-105 regions likewise flank the complete *sr2WO* genome,
262 including the eukaryotic-like *secA* [54] EAM of *WOHa2*.

263

264 *Sr3WO*. The proposed genus-level taxonomic name for *sr3WO*, described below, is *Taiwavirus*.
265 Unlike the previous groups, *sr3WO* appears to lack a conserved integration site. Rather, these
266 variants feature a core prophage region that is flanked on either side by EAM regions, are separated
267 from adjacent *Wolbachia* genes by an enrichment of transposase-encoding insertion sequences
268 (Fig 2, yellow and S4 Table), and are concentrated away from the origin of replication in the
269 bacterial chromosome (Fig 3b). While their function here is unknown, transposable Mu-like
270 phages replicate via replicative transposition in the bacterial chromosome and, much like phage
271 *WO*, are associated with severe chromosomal rearrangements and disruptions [55]. Under a similar
272 model, *sr3WO* transposases could mediate prophage replication and movement throughout the
273 *Wolbachia* genome.

274

275 Sr3WO core-prophage module synteny generally resembles that of sr2WO, although a subset of
276 variants also encode an eleven-gene module termed the *Undecim Cluster* (S4 Fig and S5 Fig),
277 discussed in detail below. Most importantly, unlike other prophage WO groups, a majority of the
278 sr3WO variants contain at least one *cifA* and *cifB* gene pair, the locus responsible for *Wolbachia*'s
279 cytoplasmic incompatibility phenotype [29, 30, 32, 46, 47].

280

281 *Sr4WO*. The prophage WO group identified strictly in *wFol* of *Folsomia candida* springtails is
282 tentatively labelled sr4WO. Unlike the above clades, sr4WO will remain unclassified at the genus
283 level due to high variability and rearrangement of the prophage genomes. A formal classification
284 will be evaluated when more genomes are sequenced that support conserved taxonomic
285 characteristics for the clade. Three variants, broken into multiple segments (S6 Fig), loosely
286 resemble the module synteny of sr3WO. WOFol1 is associated with an Undecim Cluster similar
287 to sr3WO, but all variants contain single-domain HTH_XRE genes similar to sr1WO. The sr4WO
288 prophages contain multiple genomic duplications and mobile elements [56]. While they appear to
289 lack *cifA* and *cifB* genes, they are enriched with multiple copies of *ligA* and resolvase. More
290 variants of this group are needed to analyze chromosomal integration.

291

292 **WO-like Islands**

293 We identified numerous portions of the prophage WO genome that do not contain enough genetic
294 information to be properly classified. Termed WO-like Islands, they are comprised of single core
295 phage modules, such as a baseplate or tail, and/or genes that are typically associated with the
296 prophage WO genome rather than part of the core *Wolbachia* genome (Fig 2 and S7 Fig). Most
297 WO-like Islands are therefore considered “cryptic”, “relic”, or “defective” prophages, and likely

298 originated from an ancestral prophage WO genome where they have since been domesticated by
299 the bacterial host or are in the process of degradation and elimination from the chromosome. Based
300 on studies in other systems, conserved prophage genes or gene modules that are not part of a
301 complete prophage are likely to provide a fitness advantage to their host [57, 58] and may interact
302 with, even parasitize, fully intact phages within the same bacterial host [59, 60].

303

304 Like sr3WO prophages, WO-like Islands are often flanked by at least one insertion sequence (S4
305 Table) and are commonly associated with CI genes *cifA* and *cifB*. In the unusual case of the *wIrr*
306 WO-like Island, four CI loci, along with multiple transposases, are arranged in a single genomic
307 cluster that is not associated with conserved WO genes (S7 Fig). We tentatively label the region
308 as a WO-like Island because (i) the *cif* genes and adjacent hypothetical proteins are
309 overwhelmingly associated with prophage WO regions and (ii) there is evidence of a highly
310 disrupted prophage genome about 160kb upstream in the *wIrr* chromosome (S4 Fig) that is also
311 enriched with transposases, allowing for the possibility of a prophage WO origin. Such a model
312 for the putative phage WO origin of one highly studied WO-like Island, *wMel*'s Octomom, is
313 discussed in detail below.

314

315 **Prophage WO is spatially concentrated away from the origin of replication in** 316 **the *Wolbachia* chromosome**

317 To comprehensively examine the association of each prophage WO variant with its chromosomal
318 location in *Wolbachia*, we mapped integration sites, determined by the recombinase or the most
319 5'- WO gene, on the chromosome with respect to normalized distance from the putative origin of
320 replication, *ori* [61]. There is a clustering of prophage WO insertion loci, particularly sr3WOs,

321 opposite the origin of replication (Fig 3b; Chi-square 2-tailed, $p=0.0035$) that is similar to the
322 localization patterns of temperate phages in *Escherichia*, *Salmonella*, and Negativicutes [62-65].
323 WO chromosomal location patterns support a model in which prophage insertions and WO-like
324 Islands may not be tolerated in regions directly surrounding the origin of replication.

325

326 **Transposable elements may facilitate transposition and domestication of** 327 **prophage WO regions**

328 In addition to specific chromosomal integration patterns, we next surveyed the relationship
329 between WO and its associated mobile elements. With the exception of WOCauB3, all fully
330 sequenced prophage WO genomes and WO-like Islands contained at least one transposable
331 element beyond the phage recombinase. The diversity of the WO-associated transposable elements
332 by prophage variant is listed in S4 Table and includes (i) transposases of insertion sequence
333 families IS3, IS4, IS5, IS6, IS66, IS110, IS256, IS481, IS630, IS982; (ii) recombination-promotion
334 nuclease (Rpn), which encodes a PD-(D/E)XK nuclease family transposase; and (iii) reverse
335 transcriptase of group II intron origin (RT). WO's transposable elements are associated with the
336 genomic rearrangement (e.g., WORiC), degradation or domestication (e.g., WORiA), and copy
337 number variation (e.g., WORiB) of various prophage genomes. As discussed above, flanking
338 transposases of sr3WO variants may also play a role in replicative transposition similar to phage
339 Mu.

340

341 We observed that reverse transcriptases of group II intron origin (RT) are associated with
342 chromosomal rearrangements, insertions, and/or duplications of multiple sr3WO and sr4WO
343 prophages (illustrated in S9 Fig). Likewise, we identified numerous associations of *cifA;B* gene

344 pairs with RTs of sr3WO variants (including WOPip1, WOVitA4, WOIrr, WOHal, WORiB,
345 WOAnaB, WOSuziB) and the *wIrr* WO-like Island. Therefore, the association of CI loci with
346 transposable elements – both within and beyond prophage regions – could be indicative of post-
347 integration genomic rearrangement and/or domestication of the genes, as previously discussed [6].
348 Below we propose a detailed model and evidence for the most intriguing RT-associated genomic
349 rearrangement, the origin of *wMel*'s Octomom from prophage WOMelA to generate a WO-like
350 Island (Fig 4).

351

352 **Fig 4. Comparative genomics supports a WO:Octomom origin model for *Wolbachia* proliferation in *wMelPop*.**

353 (a) A new model for Octomom origin predicts the initial infection of *wMel* with a WOMelA phage. After integration,
354 Octomom splits from the WOMelA core prophage region to form a WO-like Island. (b) A genome map of the putative,
355 intact, ancestral WOMelA where Octomom is highlighted in yellow and the extant WOMelA genome in teal illustrates
356 placement of Octomom in the WO EAM. (c-d) An alignment of the WO-PC2 region with closely related prophages
357 shows that half of the conserved module (WD0507-WD0508) is now associated with Octomom and the other half
358 (WD0257-WD0254) remained with WOMelA prophage region. DUF2466 is split across the genomic regions and,
359 when concatenated, shares homology to intact DUF2466 genes of WO-PC2. An IS5 insertion (d) is associated with
360 single-copy Octomom stability in the *wMel* chromosome. In *wMelCS*-like genomes, where the flanking RTs are intact
361 (see S10 Fig), Octomom varies in copy number. (e) When Octomom (orange-yellow) and Octomom-like (green,
362 defined by homology to WD0512, WD0513 and WO-PC2 and illustrated in S10 Fig) regions exist in a single copy,
363 either within or outside the corresponding prophage region, *Wolbachia* proliferation is normal, and it is non-
364 pathogenic. (f) If the WO-like Island occurs in multiple copies or is absent from the genome, *Wolbachia* over-
365 proliferate and are pathogenic. (*) Restoring the 1:1 (WO:Octomom) ratio returns the *wMelPop* phenotype back to
366 normal levels. The association of Octomom with pathogenicity (i.e., correlation vs. causation) is still to be determined
367 [66-68]. NCBI accession numbers are listed for each genome; (†) indicates circular genomes are unavailable and
368 genomic locations are putative.

369

370 **Unique characteristics of prophage WO**

371

372 **The WO-Octomom Model posits that Octomom is derived from the EAM;** 373 ***Wolbachia* proliferation may be dependent upon a 1:1 ratio of Octomom :** 374 **prophage WO**

375 Octomom is a cluster of eight genes in the *D. melanogaster* *wMel* *Wolbachia* genome that has
376 been described for its resemblance to a bacterial pathogenicity island (see S10 Fig for genome
377 schematic) [69]. Increasing the environmental temperature of flies either containing multiple
378 copies or completely lacking this region results in *Wolbachia* over-proliferation and pathogenicity
379 [67, 68]. Based on our observations of RT-associated genomic rearrangement, we present a new
380 WO-Octomom Model (Fig 4a) with genomic evidence (Fig 4b-d), in which Octomom putatively
381 originated from the EAM of ancestral WOMe1A (sr3WO). First, an ancestral phage WOMe1A with
382 core phage genes as well as an Octomom-encoding EAM infects *wMel* and integrates into the
383 bacterial chromosome. Second, Octomom splits from the prophage EAM region, possibly
384 mediated by RTs, to form an independent WO-like Island about 38kb from the extant WOMe1A
385 (Fig 4a). This is supported by gene synteny of the WO-PC2 variant that is split between Octomom
386 and WOMe1A at the DUF2466 gene (also annotated as *radC*). Notably, by concatenating the two
387 regions at Octomom's WD0507 (5'-DUF2466) and WOMe1A's WD0257 (3'-DUF2466), the gene
388 synteny forms a complete WO-PC2 and closely resembles that of related sr3WO prophages (Fig
389 4b-d).

390

391 Furthermore, Octomom homologs of the two-domain HTH_XRE transcriptional regulator
392 (WD0508) are characteristic of sr2WO and sr3WO prophages, and the *mutL* paralog (WD0509)

393 from Octomom is a phage WO-specific allele [70] that is distinct from the chromosomal *mutL*
394 (WD1306). This supports an ancestral WOMelA prophage genome comprised of core structural
395 modules and an Octomom-containing EAM with intact WO-PC2 (Fig 4b). An alternative
396 explanation could be that genes WD0512-WD0514 existed as a pathogenicity island in the
397 *Wolbachia* chromosome prior to WOMelA infection and later acquired adjacent EAM genes from
398 the prophage to form a complete Octomom Island. In this case, we would expect to find at least
399 one other instance of WD0512-WD0514 occurring independent of prophage regions in other
400 *Wolbachia* strains. Instead, the only *Wolbachia* homologs, to date, are associated with the EAMs
401 of WOPip5 and the wSYT (*Wolbachia* of *Drosophila santomea*, *D. yakuba*, and *D. teissieri*,
402 respectively) prophages [6, 19, 71] (S10 Fig).

403

404 An interesting and robust correlation of this WO-Octomom Model is that one copy relative to
405 prophage WO, either within or outside of the prophage region, is always a distinguishing factor of
406 non-pathogenic *Wolbachia* (Fig 4e), while absence *or* multiplication of Octomom are notably
407 associated with *Wolbachia* over-proliferation and pathogenicity (Fig 4f). This has been previously
408 reported in context of the *Wolbachia* chromosome [66, 67], and we make the distinction here of a
409 *prophage* association to enable a more fine-tuned exploration of Octomom biology. For example,
410 the disruption (*wMel*) or absence of one (*wSYT*) or both (*wPip*) flanking RTs correlates with a
411 static 1:1 ratio of the Octomom-like region (i.e., containing WD0512-WD0513 and a
412 transcriptional regulation gene) and its corresponding prophage genome (Fig 4e). Conversely, the
413 region is flanked by identical RTs on either side in all *wMel* clade VI strains, including *wMelCS*
414 and the dynamic *wMelPop* that ranges from 0 to multiple copies of the WO-like Island (Fig 4f;
415 *wMel* phylogeny presented in [66, 72]). When the 1:1 ratio in clade VI strains is disrupted, possibly

416 in conjunction with flanking RTs, *Wolbachia* develops a pathogenic relationship with its animal
417 host [66, 72]. The possible association of RTs with Octomom copy number is also notable due to
418 the observed dependence of both RT activity [73, 74] and *wMelPop* pathology [67, 68] on
419 environmental conditions, such as temperature. The direct role of Octomom on host phenotype is
420 a subject of debate [66, 67], and understanding the association of prophage WO with this region,
421 if any, could inform the biology of this unique system. The two phage-derived regions, for
422 example, may share a common regulatory mechanism since the proposed ancestral splitting of
423 Octomom from WOMelA broke a cluster of transcriptional regulators, namely one transcriptional
424 regulator (WD0508) from the other two (WD0254 and WD0255) that would typically form an
425 intact module. Alternatively, a split of Octomom from its associated prophage genome may
426 influence epigenetic modifications via WOMelA's adenine methylase (WD0267; see [66] for a
427 discussion of epigenetic vs. genetic factors).

428

429 **Undecim Cluster is a unique eleven gene island associated with prophage WO**

430 Another “pathogenicity island” candidate in the *Wolbachia* chromosome is a highly conserved set
431 of genes (WD0611 to WD0621; Fig 5a) defined here as the *Undecim Cluster* (*Undecim* is Latin
432 for “eleven”). We identify it in the majority of WO-containing *Wolbachia* genomes (Fig 1b),
433 particularly in association with *cifA*- and *cifB*-encoding regions of sr3WO (S4 Fig and S5 Fig) and
434 WO-like Islands (S7 Fig). Unlike sr3WO prophages themselves, however, the Undecim Cluster
435 does not occur more than once per *Wolbachia* genome. Its complete absence from both *wPip* and
436 *wRec* suggests that it is not strictly required for *Wolbachia*'s intracellular survival and/or ability
437 to induce cytoplasmic incompatibility. Rather, it may contribute to variation in host-symbiont
438 interactions [18, 48] by encoding a broad spectrum of metabolic functions and transport potential

439 [75, 76], including cellular exopolysaccharide and/or lipopolysaccharide (LPS) biosynthesis
440 (WD0611-WD0613; WD0620), methylation (WD0613-WD0614; WD0621), production and
441 export of antibiotics and cytotoxic compounds (WD0615-WD0616) and metabolite transport and
442 biosynthesis (WD0617-WD0619) (Fig 5b). It was identified in phage particle genomes from both
443 *w*VitA and *w*CauB [39], indicating that the region may be transferred between *Wolbachia* strains
444 via the phage. In addition, both RNA-SEQ [77] and mass spectrometry data [75] show that the
445 region is highly expressed. Interestingly, ten of the eleven genes were involved in a lateral gene
446 transfer event between *Wolbachia* and the *Rickettsia* endosymbiont of *Ixodes scapularis* (REIS;
447 [17, 76]) with WD0612 to WD0618 sharing 74% nucleotide identity to a region of the Rickettsial
448 plasmid pREIS2 and WD0619 to WD0621 sharing 67% identity to a region of the bacterial
449 chromosome (Fig 5a). We also identified homologs in *Cardinium hertigii* cHgTN10 (CP029619.1;
450 67% nucleotide identity) and *Phycorickettsia trachydisci* (CP027845.1; 68% nucleotide identity).
451 While not contiguous in *C. hertigii*, adjacent transposases may have facilitated post-integration
452 rearrangement.

453

454 **Fig 5. The Undecim Cluster contributes a wide range of cellular processes associated with host-symbiont**
455 **interactions.** (a) A genome map illustrates prophage WO's Undecim Cluster. Gene labels UC1 - UC11 correlate with
456 *w*Mel locus tags WD0611-WD0621. Lines under the genes indicate lateral gene transfer events of this region between
457 *Cardinium hertigii* cHgTN10, *Phycorickettsia trachydisci*, and multiple strains of *Rickettsia*, including the *Rickettsia*
458 endosymbiont of *Ixodes scapularis* (REIS) and its plasmid (pREIS2). Nucleotide identity is listed to the right. Dashed
459 lines indicate that the region is not contiguous in the genome. UC1 shares partial homology with a core *Wolbachia*
460 gene, *glmU* (WD0133) and was either not involved in the transfer event or has since been lost from non-*Wolbachia*
461 genomes. (b) A cellular model illustrates the putative functions associated with this region. Cellular reactions are
462 highlighted in boxes and membrane transporters are drawn as ovals. *Wolbachia* genes are labeled in blue; Undecim
463 Cluster genes are labeled in red. UC3 (WD0613) is a fusion protein with an N-terminal glycosyltransferase and C-

464 terminal radical SAM domain; therefore, it is listed twice. Reactions in light gray are likely precursors to multiple
465 pathways in glycosylation, exopolysaccharide biosynthesis, cell division, and/or virulence. Light blue is associated
466 with methylation; dark gray is associated with the production and export of antibiotics and cytotoxic compounds; and
467 navy blue is associated with metabolite transport and biosynthesis. The above functions are predicted based on
468 annotation and homology to other systems. Given the contiguous conservation of the Undecim Cluster throughout
469 prophage WO, all functions, including those not captured in this model, are likely interrelated and influence host-
470 symbiont dynamics.

471

472 **Phage WO putatively harbors a novel lytic cassette**

473 The most direct impact on *Wolbachia* cellular biology is the potential for phage WO to induce cell
474 lysis [34, 78]. The mechanism of phage-induced cell lysis has been well documented and generally
475 involves a three-component lysis system in gram-negative infecting phages: endolysin, holin, and
476 spanins [79]. This genetic system is noticeably absent from prophage WO genomes, and
477 peptidoglycan, the bacterial target of canonical phage endolysins, has never been detected in
478 *Wolbachia* [80]. We therefore hypothesized that WO phages encode an alternative lytic pathway.
479 The top candidate is a putative and novel patatin-based lytic cassette immediately upstream from
480 the tail module [81].

481

482 The cassette contains a patatin-like phospholipase A₂, a small holin-like protein, and an ankyrin-
483 repeat protein. A few prophage WO variants (i.e., WOVitA1, WOAuB, WOPip1, WOPip4, and
484 WOPip5) additionally encode an endonuclease of the phospholipase D family. Patatin-like
485 proteins determine virulence in multiple gram-negative bacteria and specifically facilitate
486 disruption of host cell membranes by *Pseudomonas aeruginosa* and *Rickettsia typhi* [82, 83]. They
487 are significantly more common in pathogenic bacteria and symbionts than in non-pathogens,

488 suggesting a role in host-association [84]. Holins are not easily annotated because they do not share
489 conserved domain sequence homology, yet several lines of evidence suggest the small protein
490 adjacent to patatin is a “holin-like” candidate: it (i) encodes a single N-terminal transmembrane
491 domain with no predicted charge; (ii) features a C-terminal coiled coil motif; (iii) is smaller than
492 150 amino acid residues; and (iv) has a highly charged C-terminal domain (S11a Fig) [79, 85, 86].
493 In addition, homologs of this holin-like gene in prophages from bacterial chromosomes other than
494 *Wolbachia* (e.g., a Tara Oceans Prophage and *Holospira* sp.) are directly adjacent to a GH108
495 lysozyme, further supporting its holin-like potential (S11b and S11c Fig, Fig 6). The third
496 conserved gene in this module, an ankyrin repeat protein with a C-terminal transmembrane
497 domain, may have the potential to impact membrane stability similar to spanins of the traditional
498 phage lysis model; alternatively, they may play a role in evasion of the arthropod-host immune
499 response similar to those in sponge-associated Ankyphages [42]. Together, this module is fairly
500 conserved across tailed WO phages and is a likely candidate in the exit and/or entry of phage
501 particles through *Wolbachia*'s multiple membranes.

502

503 **Other prophage genes in the *Wolbachia* chromosome are Gene Transfer Agents** 504 **(GTAs)**

505 In addition to prophage WO, we identified several non-WO prophage genes (S12 Fig) in the
506 majority of *Wolbachia* Supergroups, including those of the filarial nematodes. Similar to the well-
507 studied GTA of *Rhodobacter capsulatus* (RcGTA; [87, 88]), at least six of these genes encode *E.*
508 *coli* phage HK97-like conserved domains (S5 Table). We also identified GTA terminase genes
509 associated with the *Wolbachia* chromosome. As reported for *Rickettsiales*, the GTA loci are found
510 in multiple locations across the genome rather than organized in an identifiable prophage-like

511 cluster [89]. To investigate the evolutionary relationship of the GTA genes with their *Wolbachia*
512 host, we performed individual nucleotide alignments and recovered two highly conserved genetic
513 groups that demarcate Supergroup A and B *Wolbachia* (S13 Fig), supporting vertical descent with
514 modification across these major supergroups. While absent from Supergroups J and L of
515 nematodes, they are present across all other *Wolbachia* Supergroups as well as the closely related
516 genera *Candidatus Mesenet*, *Anaplasma*, *Ehrlichia*, and *Rickettsia* (S12b Fig). These results imply
517 that *Wolbachia*'s GTA genes are vertically inherited, codiverge with their bacterial hosts, and
518 likely functional given their intact sequences. They are, however, distinct from phage WO, not
519 indicative of former WO-infections, and may be lost during genome reduction.

520

521 **Prophage WO beyond *Wolbachia***

522

523 **Prophage WO-like variants occur in diverse bacterial endosymbionts and** 524 **metagenomes**

525 We identified multiple prophage WO-like variants beyond the *Wolbachia* genus that have gene
526 synteny and nucleotide identity to prophage WO structural modules in: (i) endonuclear bacterial
527 symbionts of *Paramecium* (*Holospora obtusa*, *H. undulata*, *H. elegans*, and *H. curviuscula*) [90];
528 (ii) metagenome projects from an advanced water treatment facility [91], the Indian Ocean (*Tara*
529 Oceans circumnavigation expedition [92]), and a marine aquaculture habitat [93]; (iii) *Candidatus*
530 *Mesenet longicola*, the CI-inducing bacterial endosymbiont of *Brontispa longissima* [94]; and (iv)
531 multiple strains of *Orientia tsutsugamushi* isolated from humans (Fig 6a). While the structural
532 genes closely resembled those of prophage WO, novel genes were identified in the
533 replication/repair and lysis modules (Fig 6a, genes with prophage WO homology are highlighted

534 in yellow). All non-*Wolbachia* variants except *Candidatus Mesenet longicola* lacked signature
535 *Wolbachia* phage WO genes such as patatin, ankyrin repeats, and the EAM that are putatively or
536 definitively involved in phage-by-arthropod interactions.

537

538 **Fig 6. WO-like prophage regions are found in endonuclear *Paramecium* endosymbionts, aquatic environments,**
539 **and other animal-associated bacteria.** (a) Genome maps of non-*Wolbachia* prophage regions illustrate similar gene
540 content and synteny to prophage WO. Locus tags are listed in italics above the genes; NCBI contig accession numbers
541 are shown in the right-hand corner of each genome. Dashed lines represent breaks in the assembly whereas small
542 diagonal lines represent a continuation of the genome onto the next line. Genes with nucleotide homology to prophage
543 WO are highlighted in yellow and genes of similar function are similarly color-coded according to the figure legend.
544 *Candidatus Mesenet longicola* is the only genome to feature EAM genes, including *cifA* and *cifB*. Arrows with
545 diagonal stripes represent genes that may be pseudogenized relative to homologs in other prophage genomes. Genome
546 maps for *H. elegans* and *H. curviuscula* prophages are not shown. (b) WO-like Islands featuring tail and lysis genes
547 share homology with the *Orientia* regions and may represent phage-derived bacteriocins. Predicted physical structures
548 are illustrated to the left of each genome. Images illustrate the isolation source for each prophage: green borders
549 represent protozoa; blue borders represent aquatic environments; gold borders represent animals.

550

551 Relative to the full-length genomes recovered from *Holospora*, *Candidatus Mesenet longicola* and
552 the metagenome projects, *Orientia* prophages appeared to be highly degenerate. These regions
553 featured only tail and lysis genes, but the modules are noticeably intact. Some WO-like Islands,
554 such as WOAlbB2, WONO4, and WOMau3 (Fig 6b), also harbor sole tail and lysis modules. The
555 retention of a complete phage structural module in the bacterial chromosome suggests that it has
556 been domesticated and adapted to benefit the host. For example, several studies report phage-
557 derived bacteriocins that consist of tail and lysis genes and target other strains of the same bacterial
558 species [57]. Similarly, an extracellular contractile injection system (eCIS) comprised of phage

559 tail-like proteins specifically targets eukaryotic cells [95]. Overall, the presence of WO-like
560 variants in non-*Wolbachia* genera continue to support phage WO lateral transfer between
561 unrelated, coinfecting symbionts. This is further evident by the presence of the CI genes, *cifA* and
562 *cifB*, in the *O. tsutsugamushi* genome [96], which may represent a derived variant of phage WO
563 from *Wolbachia* that has since been domesticated by its bacterial host. Alternatively, the
564 association of CI genes in a bacterium harboring WO-like variants could be indicative of two other
565 possible origins - either the last common ancestor of the WO and WO-like phages encoded *cifA*
566 and *cifB*, or the loci may have originated in WO-like phages and transferred to *Wolbachia*. For
567 divergent, horizontally transferred elements, it is often not possible in practice to assign a direction
568 of evolution and origin story.

569

570 **Linnaean classification of phage WO**

571

572 Finally, while phage WO is a model organism to study the tripartite association between viruses,
573 endosymbiotic bacteria, and animal hosts, it is not yet recognized by the International Committee
574 on Taxonomy of Viruses (ICTV). Recently, the ICTV Executive Committee implemented a
575 pipeline for the official classification of viruses from metagenomic datasets [45], including those
576 originating from integrated prophage sequences. Through our comparative analysis of prophage
577 WO sequences here with those that have been sequenced from active particles (i.e., WOVitA1 and
578 WOCauB3), we propose a formal phage WO taxonomy (Fig 7) to align with the ICTV Linnaean-
579 based classification code [44]. The correlation between common name and proposed scientific
580 name for each taxonomic rank is listed in Table 1.

581

582 **Fig 7. Comparative genomics supports a new order-level designation for prophage WO classification.**

583 Symbiovirales is proposed as a new taxonomic order of tailed phages within the class *Caudoviricetes*. It contains
 584 viruses that primarily infect *Wolbachia* (proposed family Woviridae) and other symbionts (proposed family
 585 Holoviridae). Two proposed subfamilies, Kuehnivirinae and Pipivirinae, distinguish the sr1WO/sr2WO and sr3WO
 586 clades (Figs 2 and 3, respectively). Three proposed genera of Woviridae include Cautellavirus (sr1WO), Vitrivirus
 587 (sr2WO), and Taiwavirus (sr3WO). sr4WO prophages are currently unclassified. Holoviridae contains a single
 588 proposed genus, Paramecivirus, that encompasses closely related prophages of *Holospira* and metagenome-
 589 assembled genomes (MAGs) from aquatic environments.

590

591 **Table 1.** The correlation between common name and proposed scientific name is listed for each phage WO exemplar
 592 variant and taxonomic rank.

WO Exemplar Variant	Taxonomic Rank	Common Name	Proposed Scientific Name
WOCauB3	Species	WOCauB3	<i>Wolbachia</i> virus WOCauB3
	Genus	sr1WO	Cautellavirus
	Subfamily	N/A	Kuehnivirinae
	Family	Phage WO	Woviridae
	Order	WO-like viruses	Symbiovirales
WOVitA1	Species	WOVitA1	<i>Wolbachia</i> virus WOVitA1
	Genus	sr2WO	Vitrivirus
	Subfamily	N/A	Kuehnivirinae
	Family	Phage WO	Woviridae
	Order	WO-like viruses	Symbiovirales
WOMelB	Species	WOMelB	<i>Wolbachia</i> virus WOMelB
	Genus	sr3WO	Taiwavirus
	Subfamily	N/A	Pipivirinae
	Family	Phage WO	Woviridae
	Order	WO-like viruses	Symbiovirales

593

594 We propose that all phage WO and WO-like viruses be classified in existing class *Caudoviricetes*
 595 (phylum *Uroviricota*; kingdom *Heunggongvirae*; realm *Duplodnaviria*) for tailed phages based
 596 on the presence of a tail module and observed tail-like structure in electron microscopy [34, 78].

597 We propose the new order Symbiovirales to recognize the association of these viruses with
598 endosymbionts. Two proposed families, Woviridae and Holoviridae, are named after the first
599 bacterial host identified for each family (*Wolbachia* endosymbionts of arthropods and *Holospora*
600 endonuclear symbionts of *Paramecium*, respectively). Modules shared across the proposed
601 Symbiovirales order are recombinase, replication, head, connector/baseplate, tail fiber, tail, and a
602 putative lytic cassette (See Fig 8 for a summary of taxonomic traits).

603

604 **Fig 8. Linnaean classification of prophage WO-like viruses is supported by taxonomic traits at the order,**
605 **family, subfamily, and genus level.**

606 (a) Proposed order Symbiovirales encompasses viruses that infect symbiotic bacteria, contain a large serine
607 recombinase for integration and a PAAR gene in the connector/baseplate module, and feature a conserved set of core
608 phage modules. They share nucleotide homology to *Wolbachia*'s prophages. (b) Subfamilies are classified by presence
609 (Woviridae) or absence (Holoviridae) of an EAM and ankyrin repeat containing proteins. Woviridae may utilize
610 patatin for lysis whereas Holoviridae encode a canonical GH108 endolysin. (c) Two proposed subfamilies address the
611 diversity of chromosomal integration patterns and EAM location of prophages within the Woviridae family. (d)
612 Proposed genera are further distinguished by multiple factors including structural module synteny, HTH_XRE
613 domains, and genome composition.

614

615 The suggested family Woviridae encompasses all phage WO and prophage WO variants and is
616 distinguishable by the presence of EAM and eukaryotic-like genes, a patatin-like phospholipase,
617 and multiple ankyrin repeat containing proteins (Fig 8). Upon ICTV approval, Woviridae will be
618 split into two subfamilies - Kuehnivirinae and Pipivirinae - named after the first purification of
619 phage WO particles from *Ephestia kuehniella* [37] and *Culex pipiens* [35], respectively.

620

621 The proposed Kuehnivirinae will encompass two genera for phages that integrate into discrete *att*
622 sites and feature 3'-placement of the prophage EAM. The first suggested genus of this subfamily,
623 Cautellavirus, recognizes the sequenced genomes from *wCauB* phages [37, 38] and encompasses
624 all *sr1WO* prophages (Fig 7). Cautellavirus core module synteny (replication, head,
625 connector/baseplate) is inverted relative to other members of the proposed Woviridae; the ankyrin
626 located between the tail module and putative lytic cassette is encoded on the opposite strand; and
627 the genome does not contain a methylase/ParB protein (S1 Fig). The second suggested genus of
628 this subfamily, Vitrivirus, recognizes the first fully sequenced genome from phage WOVitA1
629 particles [39] and encompasses all *sr2WO* prophages (Fig 7). Members of this genus feature
630 discrete integration into the VNTR-105 locus, and the recombinase is adjacent to ankyrin repeats
631 rather than WO-PC1.

632
633 Members of the proposed subfamily Pipivirinae are currently not associated with distinct *att* sites
634 and are often flanked by EAM-like genes and transposases (S4 Table) on both ends of the
635 integrated genome. Pipivirinae contains only one genus, Taiwavirus, named after the first prophage
636 WO sequence fragment from *wTai* [3, 78]. The proposed genus Taiwavirus will encompass all
637 *sr3WO* prophages (Fig 7) and is the most speciose genus of Symbiovirales. Likewise, it also
638 features the greatest number of degraded prophage regions both within and across diverse
639 *Wolbachia*. As more prophages are sequenced, it may be prudent to further classify this clade into
640 subgenera based on presence or absence of the Undecim Cluster (Fig 2).

641
642 Finally, the WO-like prophages of *Candidatus Mesenet longicola* are likely classified as
643 Woviridae due to nucleotide homology of structural genes and the presence of *cifA;B* containing

644 EAM, but complete sequence information (specifically the recombinase and 5'-region beyond the
645 CI loci) is necessary to definitively classify these phages. Likewise, the *wFol* prophages will
646 remain as *Unclassified* Woviridae until more genomes are sequenced to provide definitive
647 taxonomic characteristics for the sr4WO variants. As more prophage WO genomes are sequenced,
648 we propose using the srWO designation as a “common name” that roughly correlates with genus-
649 level demarcation and referencing srWO when proposing future additions to the Woviridae
650 taxonomy.

651

652 The proposed family Holoviridae includes the WO-like prophages from most non-*Wolbachia*
653 metagenomic sequences and is currently comprised of phages from aquatic endosymbionts. They
654 lack an EAM and ankyrin repeat containing proteins, feature a GH108 hydrolase rather than
655 patatin-like phospholipase in the putative lytic cassette, and encode LexA and YqaJ that are
656 generally absent from *Woviridae* genomes (Fig 6). Due to gene synteny and sequence homology
657 of these prophage genomes, all species are currently classified into a single Paramecivirus genus.
658 The first representatives of this genus were identified in *Holospira* spp., endonuclear symbionts
659 of *Paramecium caudatum* and *P. bursaria* [97].

660

661 In summary, we propose that viruses should be classified as Symbiovirales based on reciprocal
662 BLAST homology and shared gene content with core phage WO. The large serine recombinase
663 can be used as a typing tool (Fig 3a) and intact genomes for inclusion should include (i)
664 recombinase, (ii) replication and repair, (iii) connector/baseplate, (iv) tail fiber, (v) tail, and (vi)
665 lytic modules. Woviridae are delineated by the presence of a eukaryotic association module
666 (EAM), multiple ankyrin repeats, and a patatin-containing lytic module. Holoviridae are

667 characterized by the absence of an EAM, lack of ankyrin repeats, and a GH108-containing lytic
668 module.

669

670 **Discussion**

671 The survey of 150 genomes coupled with manual annotations and comparative sequence analyses
672 offers the most comprehensive overview of *Wolbachia* prophage WO genomics, distribution, and
673 classification to date. From these analyses, we propose four major prophage WO variants
674 corresponding with genus-level Linnaean taxonomy and support the creation of a new order
675 Symbiovirales (within the *Caudoviricetes*) containing two distinct families, Woviridae and
676 Holoviridae. Results presented above suggest that tailed, intact prophage WO genomes serve as a
677 proxy for estimating prophage autonomy vs. domestication in the *Wolbachia* genome where
678 multiple “degraded” prophages and WO-like Islands are indicative of prophage WO domestication
679 by the bacterial host. WO regions enriched with transposable elements contribute to genome
680 plasticity of the bacterial chromosome and may play a role in the domestication of these prophages.
681 One such region, Octomom, has a putative WO origin in which a former EAM region is
682 dynamically replicated or eliminated, and is associated with pathogenicity when not in a 1:1 ratio
683 with its ancestral prophage. Finally, while there is currently no transformation system for
684 *Wolbachia*, future applications may take advantage of conserved integration loci associated with
685 each srWO and utilize the serine recombinase to introduce new genetic material into the bacterial
686 chromosome.

687

688 **Establishment of the prophage WO database**

689 To assist future analyses of prophage WO, a database of genomes discussed in this study is publicly
690 available at <https://lab.vanderbilt.edu/bordenstein/phage-wo/>. The Prophage WO Database
691 features sequence data, enhanced annotations, and phylogenetic tools to support: (i) identification
692 of prophage WO regions in newly assembled *Wolbachia* genomes; (ii) annotation of the Undecim
693 Cluster, cytoplasmic incompatibility (*cif*) genes, putative EAM genes, WO-PC2, and other WO-
694 associated regions; and (iii) taxonomic classification of prophage WO-like viruses.

695 **Methods**

696

697 **Prophage WO genome maps and chromosomal integration patterns**

698 Prophage WO regions were manually retrieved from sequenced *Wolbachia* genomes in GenBank
699 via BLASTN searches against each individual *Wolbachia* genome in the Nucleotide (NR/NT) and
700 WGS databases [43]. Genomes from WOCauB3, WOVitA1, WOMelB, WOPip5, and WOFol3
701 were the primary reference genomes used for each search. Because most prophage regions were
702 incomplete and located at the ends of contigs, we selected more complete assemblies for
703 comparative genomics: *w*Ri, *w*Ana, *w*Suzi, *w*VitA, *w*Ha, *w*Mel, *w*Pip, *w*No, *w*Au, *w*Irr, *w*Fol,
704 *w*AlbB, *w*Mau, and the previously described prophage genomes WOKue, WOCauB2, WOCauB3,
705 WOSol, WOREcA, and WOREcB (See S1 Table for accession numbers). All genomes were
706 reannotated in Geneious Prime v2019.2 using the InterProScan [98] plug-in along with information
707 from BLASTP [99], Pfam [100], HHPRED [101], ISFinder [102], and SMART [103] databases.
708 Prophages were then organized into groups based on similar gene content and module
709 organization. Whole genome alignments were performed with the Mauve [104] plug-in in
710 Geneious.

711

712 Prophage genomic boundaries for sr1WO and sr2WO were defined by 5' and 3' homology to a
713 known *attP* site (discussed below). Prophage genomic boundaries for sr3WO and sr4WO were
714 identified by translating each prophage gene and “walking out” from the structural modules by
715 using a BLASTP of each gene product against the core *Wolbachia* genome. If a gene was identified
716 in most *Wolbachia* strains, including those infecting nematodes, as well as in the closely related
717 genera *Ehrlichia* and *Anaplasma*, it was considered a core *Wolbachia* gene and not included in the

718 prophage annotation. If a gene was only present in WO-like regions of other *Wolbachia* genomes,
719 it was considered a phage-associated gene. Because the HTH_XRE transcriptional regulators
720 (WO-PC2) were identified in phage purifications from WOCauB3 and WOVitA1, any genes
721 located between the structural modules and WO-PC2 were considered part of the prophage
722 genome. Through this method, we identified flanking 5' and 3' transposases that separated phage-
723 associated genes and the bacterial chromosome in sr3WO and sr4WO regions. Because some
724 transposable elements did not fall within the known IS Groups for *Wolbachia* [2], they were
725 comparably annotated to IS Family using ISFinder.

726

727 Chromosomal integration patterns were analyzed by similarly aligning all circular genomes based
728 on the putative origin of replication, *ori* [61]: WD1027 (CBS domain-containing)-like genes were
729 oriented in the reverse direction and WD1028 (*hemE*)-like genes were oriented in the forward
730 direction. The nt-distance from *ori* to the prophage recombinase, or 5'-gene, was divided by the
731 length of the total *Wolbachia* genome and multiplied by 100 for a % distance from *ori*. The *wVitA*
732 and *wRec* genome arrangements may not be exact as they contain multiple scaffold breaks and
733 genome orientation was estimated based on homology to closely related genomes.

734

735 **Recombinase homology and phylogenetics**

736 Large serine recombinase genes from each reference genome were translated and aligned using
737 the MUSCLE [105] plugin in Geneious. The best model of evolution, according to corrected
738 Akaike information criteria, was determined by ProtTest [106, 107] and the phylogenetic tree was
739 constructed using default parameters of the MrBayes [108] plugin in Geneious with Rate

740 Matrix=jones and Rate Variation=invgamma. A Consensus Tree was built with a support threshold
741 of 50% and burn-in of 10%.

742

743 **Phage WO *att* sites**

744 The *attP* sites for WOVitA1 and WOCauB3 were previously identified by sequencing active phage
745 particles and confirmed with PCR and Sanger sequencing [39]. Each *attP* sequence was submitted
746 as a BLASTN query against *Wolbachia* genomes harboring similar prophage haplotypes to
747 identify specific *attL* and *attR* sites. The *attB* sites were predicted by concatenating chromosomal
748 sequences adjacent to *attL* and *attR*. The predicted *attB* sites were then used as queries in a
749 BLASTN search against *Wolbachia* genomes to confirm that the sequences exist, uninterrupted,
750 in chromosomes lacking similar prophage haplotypes.

751

752 **Phage WO beyond *Wolbachia***

753 Contigs containing WO-like prophage regions in *Holospora*, *Orientia*, *Candidatus Mesenet*, and
754 multiple metagenome-associated taxa were identified by a BLASTP query of prophage WO
755 sequences against the NCBI database. The nucleotide sequence for each homolog (usually a contig
756 in the WGS database) was manually inspected for WO-like regions. If detected, the boundaries of
757 each prophage region were determined using the similar “walk out” BLASTP approach described
758 above, looking for homology to other phage or bacterial genes. All non-Anaplasmatataceae
759 prophage genomes had concise boundaries (recombinase and lysis module) that did not include an
760 EAM.

761

762 **Identification of Gene Transfer Agents**

763 The genome annotations used for comparative genomics were manually inspected for keywords
764 *phage*, *capsid*, and *tail*. Any gene not within an annotated prophage WO region was translated and
765 a BLASTP was performed against the NCBI database. Based on top hits, genes were binned into
766 “WO-like” indicating homology to phage WO and “GTA” indicating homology to HK97 phage.

767

768 **Taxonomic Classification**

769 The proposed taxonomic classification of phage WO was drafted in accordance with ICTV
770 guidelines for genome-based taxonomy [109] and will be formally reviewed by the Committee in
771 the next cycle. Specifically, it is recommended that phages should be assigned the same species if
772 their genomes are more than 95% identical; assigned the same genus if genomes share 80%
773 nucleotide identity across the genome length and form monophyletic groups based on a
774 phylogenetic tree of signature gene(s); assigned the same subfamily (optional) if they share a low
775 degree of sequence similarity and the genera form a clade in a marker tree phylogeny; assigned
776 the same family if they share orthologous genes and form a cohesive and monophyletic group in a
777 proteome-based clustering tool; and assigned the same order when two or more families are
778 related. Prophage WO taxonomic classification satisfied all demarcation criteria except for genus
779 designation. At the genus level, due to the high variability of the EAM, we applied alternative
780 criteria: genomes should (i) share >70% nucleotide homology across >30% of the genome; (ii)
781 form a distinct phylogenetic clade based on the amino acid sequence of the signature typing gene,
782 large serine recombinase; and (iii) demonstrate shared gene and module synteny.

783

784

785 **Supplementary Figures**

786

787 **S1 Fig. Cautellavirus (sr1WO) genome maps.** Genome maps of sr1WO prophage regions where
788 genes are drawn to scale in forward and reverse directions. Predicted physical structures are
789 illustrated to the left of each genome. All genomes contain tail modules with the exception of the
790 partial WOVitA2 sequence. Prophage WO Core Genes are shaded in blue and predicted EAM
791 genes are shaded in gray. Genes of similar function are similarly color-coded according to the
792 figure legend. Locus tags, if available, are listed in italics above the genes. The large, black
793 diagonal lines between the recombinase and transposase in WORiC and WOSuziC represent post-
794 integration rearrangement of the prophage region in the *Wolbachia* chromosome. Dashed lines
795 represent breaks in the assembly whereas small diagonal lines represent a continuation of the
796 genome onto the next line. Arrows with diagonal stripes represent genes that may be
797 pseudogenized relative to homologs in other prophage WO genomes. The putative function for
798 each structural gene is discussed in S1 Text.

799

800 **S2 Fig. Vitrivirus (sr2WO) genome maps.** Genome maps of sr2WO prophage regions where
801 genes are drawn to scale in forward and reverse directions. Predicted physical structures are
802 illustrated to the left of each genome. WOVitA1-like prophage genomes encode all structural
803 modules (shaded in blue) and an EAM (shaded in gray) whereas WORiA-like prophage genomes
804 encode an intact head module, recombinase, lysozyme, AAA16, and disrupted connector. They
805 lack most other modules. Genes of similar function are similarly color-coded according to the
806 figure legend. Locus tags, if available, are listed in italics above the genes. Dashed lines represent
807 breaks in the assembly whereas small diagonal lines represent a continuation of the genome onto

808 the next line. Arrows with diagonal stripes represent genes that may be pseudogenized relative to
809 homologs in other prophage WO genomes. The putative function for each structural gene is
810 discussed in S1 Text.

811

812 **S3 Fig. Taiwavirus (sr3WO) genome maps.** Genome maps of sr3WO prophage regions where
813 genes are drawn to scale in forward and reverse directions. Three *wPip* prophages exist as one
814 contiguous prophage region in the *Wolbachia* genome and are illustrated here as WOPip1,
815 WOPip2, and WOPip3 (based on [110]). Predicted physical structures are illustrated to the left of
816 each genome. Prophage WO Core Genes are shaded in blue and predicted EAM genes are shaded
817 in gray. Genes of similar function are similarly color-coded according to the figure legend. sr3WO
818 is comprised of highly variable genomes that are often flanked by mobile elements (transposases
819 are shown in yellow). They generally contain a recombinase, connector/baseplate, head, and EAM
820 with only a few genomes encoding a complete tail. Prophages in this group often contain *cifA;B*
821 (pink). Locus tags, if available, are listed in italics above the genes. Dashed lines represent breaks
822 in the assembly whereas small diagonal lines represent a continuation of the genome onto the next
823 line. Arrows with diagonal stripes represent genes that may be pseudogenized relative to homologs
824 in other prophage WO genomes. The putative function for each structural gene is discussed in S1
825 Text.

826

827 **S4 Fig. Taiwavirus (sr3WO and sr3WO-Undecim Cluster) genome maps.** Genome maps of
828 sr3WO prophage regions where genes are drawn to scale in forward and reverse directions. WOIr
829 is one contiguous prophage region in the *Wolbachia* genome that is illustrated here as Segment 1
830 and Segment 2. A subset of sr3WO prophages is further categorized by the presence of a highly

831 conserved WD0611-WD0621 like region, termed the Undecim Cluster (navy blue). Predicted
832 physical structures are illustrated to the left of each genome. Prophage WO Core Genes are shaded
833 in blue and predicted EAM genes are shaded in gray. Genes of similar function are similarly color-
834 coded according to the figure legend. sr3WO is comprised of highly variable genomes that are
835 often flanked by mobile elements (transposases are shown in yellow). Prophages in this group
836 often contain *cifA;B* (pink). Locus tags, if available, are listed in italics above the genes. Dashed
837 lines represent breaks in the assembly whereas small diagonal lines represent a continuation of the
838 genome onto the next line. Arrows with diagonal stripes represent genes that may be
839 pseudogenized relative to homologs in other prophage WO genomes. The putative function for
840 each structural gene is discussed in S1 Text.

841

842 **S5 Fig. Taiwavirus (sr3WO-Undecim Cluster) genome maps.** Genome maps of sr3WO
843 prophage regions where genes are drawn to scale in forward and reverse directions. This subset of
844 sr3WO prophages is further categorized by the presence of a highly conserved WD0611-WD0621
845 like region, termed the Undecim Cluster (navy blue). Predicted physical structures are illustrated
846 to the left of each genome. Prophage WO Core Genes are shaded in blue and predicted EAM genes
847 are shaded in gray. Genes of similar function are similarly color-coded according to the figure
848 legend. sr3WO is comprised of highly variable genomes that are often flanked by mobile elements
849 (transposases are shown in yellow). Prophages in this group often contain *cifA;B* (pink). Locus
850 tags, if available, are listed in italics above the genes. Dashed lines represent breaks in the assembly
851 whereas small diagonal lines represent a continuation of the genome onto the next line. Arrows
852 with diagonal stripes represent genes that may be pseudogenized relative to homologs in other
853 prophage WO genomes. The putative function for each structural gene is discussed in S1 Text.

854

855 **S6 Fig. Unclassified (sr4WO) genome maps.** Genome maps of sr4WO prophage regions where
856 genes are drawn to scale in forward and reverse directions. To date, sr4WO prophages have only
857 been identified in the parthenogenic strain of *Folsomia candida*, *wFol*. WOFol2 is one contiguous
858 prophage region in the *Wolbachia* genome that is illustrated here as Segment 1 and Segment 2.
859 Likewise, the WOFol3 prophage region is illustrated as three segments. Predicted physical
860 structures are illustrated to the left of each genome. Prophage WO Core Genes are shaded in blue
861 and predicted EAM genes are shaded in gray. Genes of similar function are similarly color-coded
862 according to the figure legend. Locus tags, if available, are listed in italics above the genes. Small
863 diagonal lines represent a continuation of the genome onto the next line. Arrows with diagonal
864 stripes represent genes that may be pseudogenized relative to homologs in other prophage WO
865 genomes. The putative function for each structural gene is discussed in S1 Text.

866

867 **S7 Fig. WO-like Island genome maps.** Genome maps of WO-like Islands where genes are drawn
868 to scale in forward and reverse directions. These regions contain only one structural module and/or
869 group of WO-related genes. Regions flanked by assembly breaks (i.e., WOREcB, WOREcA, and
870 *wVitA*) are tentatively classified as WO-like Islands due to lack of a full-length prophage in the
871 genome assembly. Names are based on the original author's description. If it was identified as a
872 prophage in the genome announcement, the reported WO name is listed here. Otherwise, the name
873 simply refers to the encoding *Wolbachia* genome. Many WO-like Islands contain *cifA;B*; some
874 Islands (i.e., *wNo*, *wVitA*, WOMau4, and WOAlbB3) contain both Type III *cifA;B* (pink) and the
875 Undecim Cluster (navy blue). Predicted physical structures are illustrated to the left of each
876 genome. Prophage WO Core Genes are shaded in blue and predicted EAM genes are shaded in

877 gray. Genes of similar function are similarly color-coded according to the figure legend. Locus
878 tags, if available, are listed in italics above the genes. Dashed lines represent breaks in the
879 assembly. Arrows with diagonal stripes represent genes that may be pseudogenized relative to
880 homologs in other prophage WO genomes. The putative function for each structural gene is
881 discussed in S1 Text.

882

883 **S8 Fig. *In silico* predictions of phage WO attachment (*att*) sites.** An integrated prophage
884 sequence contains left and right attachment sites (*attL* and *attR*, respectively) at the points of
885 chromosomal integration. Half of the *att* site is phage-derived (green); the other half is bacterial
886 derived (black). If the DNA sequence of the bacterial attachment site (*attB*, black) is known, a
887 nucleotide alignment of the intact sequence with the integrated prophage genome will correlate
888 with 5'- (*attL*) and 3'- (*attR*) prophage boundaries. (a) WORiC, a member of sr1WO, integrates
889 into *wRi*'s magnesium chelatase gene. By aligning an intact copy of this gene (WD0721) from
890 closely related *wMel* that does not harbor sr1WO, (b) the juncture points of the disrupted
891 magnesium chelatase indicate the *attL* and *attR* sites for the WORiC prophage region within the
892 *wRi* genome. (b) The phage attachment site (*attP*, green) is predicted *in silico* by concatenating
893 the non-*Wolbachia* portions of the *attL* and *attR* sites. (c) Likewise, this method can also be
894 applied when the bacterial integration locus is intergenic. The homologous intergenic region of
895 closely related, sr1WO-free *wPip* can be used to predict *att* sites for WOCauB3. Nucleotides in
896 orange represent a common region, O, that is shared by all four *att* sites. This method was adapted
897 from [39] where the *attP* site was used to predict the *attB* site of sr2WO phages.

898

899 **S9 Fig. RT is associated with duplication, inversion, and recombination of the prophage WO**
900 **genome.** (a) The WOMelB prophage genomes of *wMel2_a* and *wMel2_b* are duplicated relative
901 to the *wMel* reference genome [72]. (b) The entire WORiB prophage region is duplicated in *wRi*
902 [19]. (c) WOHa1 encodes a second, pseudogenized *cifA;B*-containing region relative to closely
903 related WOAuA, WORiB, WOSuziB, and WOSol prophages. (d) A ligase-containing region is
904 duplicated in *wFol*'s WOFol1 and WOFol2 [56]. (e) Based on homology to other prophage regions
905 (Fig 2), the connector/baseplate should be adjacent to a head module and the WOPC-2 and
906 replication genes should be oriented in the opposite direction; this indicates a likely insertion
907 and/or recombination in the WOFol3 prophage region. (f) The WOirr head module is inverted
908 relative to other sr3WOs. Genes are illustrated as arrows; putative gene annotations are labeled in
909 S1-S7 Figs. In each example, the regions of chromosomal rearrangement are highlighted in light
910 orange and flanked by at least one RT.

911

912 **S10 Fig. Comparative genomics of Octomom-like variants across diverse *Wolbachia*.**

913 Octomom (yellow-orange) and Octomom-like (green) regions are illustrated for *wMelCS*, *wMel*,
914 *wSYT* clade, and *wPip*. Characteristics of each region are listed next to the genome schematic.
915 Notably, the *wMelCS* genome, representative of the dynamic *wMelPop*, is distinguished from
916 other variants by intact, flanking reverse transcriptases of group II intron origin (RT) on both sides.
917 *wPip*, the only *Wolbachia* Supergroup B variant, is the most divergent and not associated with an
918 RT, MutL or ankyrin repeat. Rather it is adjacent to WP1349, another gene that has been
919 horizontally transferred between phage and arthropod [71].

920

921 **S11 Fig. Prophage WO encodes a putative lytic cassette.** Adjacent to the tail module of most
922 prophage WO variants are three phage lysis candidates: ankyrin repeat containing protein (not
923 shown), holin-like, and patatin-like phospholipase. (a) Similar to canonical holins, the prophage
924 WO gene product encodes a single N-terminal transmembrane domain with no predicted charge.
925 It is smaller than 150 amino acid residues, features a C-terminal coiled coil motif, and has a highly
926 charged C-terminal domain. Unlike canonical holins, however, it is adjacent to a patatin-like gene
927 rather than a characterized endolysin. (b) The prophage WO holin-like peptide shares 41.1% amino
928 acid identity to a homolog in the non-*Wolbachia* prophage from the Tara Oceans Project that is
929 directly adjacent to a GH108 lysozyme (complete genome illustrated in Fig 6). (c) A Mauve
930 alignment of these genomic regions (core phage modules only; EAM not included) indicates
931 50.3% nucleotide identity across the majority of the sequence, including the holin-like gene
932 (marked with a gold star). The similarity of these prophages suggest that prophage WO may utilize
933 a similar holin-like gene with a different lytic enzyme (i.e., patatin rather than lysozyme) to lyse
934 the bacterial cell.

935

936 **S12 Fig. *Wolbachia* contains both prophage regions and GTA-like genes scattered through**
937 **the chromosome.** (a) Circular *w*Mel contains three prophage WO-like regions (teal) and multiple
938 genes with homology to GTAs (orange) scattered throughout the genome, illustrated relative to
939 the putative origin of replication (*ori*, gray). The Undecim Cluster is highlighted in navy blue,
940 *cifA;B* are highlighted in pink, and *wmk* is highlighted in purple. (b) GTAs are present in at least
941 one strain of each *Wolbachia* Supergroup except Supergroups J and L. They are also present in
942 closely related Anaplasmataceae genera.

943

944 **S13 Fig. Distance matrices of GTA nucleotide homology indicate evolution with the**
945 ***Wolbachia* chromosome.** Nucleotide alignments of GTA genes (a) portal, (b) BRO599, (c) TIM
946 barrel, (d) major capsid, (e) head-tail connector, and (f) terminase indicate strict delineation based
947 on *Wolbachia* supergroup. This supports evolution with the *Wolbachia* chromosome rather than
948 independent evolution of a phage genome.

949

950 **Supplementary Tables**

951

952 **S1 Table. Prophage WO genes are associated with arthropod-infecting *Wolbachia*.** *Wolbachia*
953 genomes are listed according to (A) host phylum; (B) *Wolbachia* supergroup; (C) *Wolbachia* name
954 (D) host species and (E) host strain/lineage, if applicable; (F) NCBI accession number; (G) genome
955 assembly status; (H) identification of prophage WO core genes; (I) identification of CI genes; and
956 (J) identification of the Undecim Cluster. *Wolbachia* strains that did not include official names in
957 the assembly reports are listed here using a capital letter for host genus and two to three lowercase
958 letters for host species. “Highly pseudogenized” in column H indicates that the prophage genome
959 is highly pseudogenized and encodes very few Core WO genes. (*) indicates that the genome lacks
960 a complete Undecim Cluster but encodes WD0616 and/or WD0621 homologs. (**) indicates that
961 the genome was not included as Source Data for Fig 1b due to incomplete genome information.

962

963 **S2 Table. *wMhie* encodes prophage WO genes.** *wMhie*, a *Wolbachia* endosymbiont from the
964 nematode *Madathamugadia hiepei*, encodes four genes that are conserved throughout phage WO’s
965 transcriptional regulation and replication/repair modules. Each gene is listed by locus tag,
966 annotation, and nucleotide homology to prophage WOVitA1.

967

968 **S3 Table. *cifA* and *cifB* genes are associated with *Wolbachia* Supergroups F and T.** *cifA* and
969 *cifB* are identified in Supergroups F and T. NCBI accession numbers and genomic coordinates (or
970 locus tags) are provided for each locus.

971

972 **S4 Table. Diversity of prophage WO mobile elements.** All mobile elements, both flanking and
973 internal, are listed for each prophage WO genome according to original genome annotations and
974 ISFinder [102]. The sr1WO group and WOVitA1-like prophages of the sr2WO group do not
975 feature transposases on the 5'- and 3'- flanking regions. The WORiA-like prophages of the sr2WO
976 group are associated with 3'- transposases; these correlate with putative truncations of the
977 prophage regions. Most genomes within the sr3WO group feature mobile elements on both 5'- and
978 3'- ends. IS refers to Insertion Sequence Family; RT refers to reverse transcriptase of group II
979 intron origin; Rpn refers to recombination promoting nuclease. (*) indicates a sequencing gap or
980 artificial join in the *Wolbachia* genome. Complete sequence information is unknown. (**)
981 indicates that these prophage sequences were obtained from contigs and may be segmented in the
982 *Wolbachia* chromosome; the exact 5' and 3' ends are uncertain. Genomic locations for each mobile
983 element are illustrated in S1-S7 Figs.

984

985 **S5 Table. *Wolbachia* GTA genes.** The annotation of *Wolbachia*'s distributed GTA genes is based
986 on a BLASTP against NCBI Conserved Domains; E-values are listed in column B.

987

988

989 **Supplementary Text**

990

991 **S1 Text: Phage WO Structural Modules.**

992 Phage WO structural genes are organized into head, connector/baseplate, tail, and tail fiber
993 modules. The predicted function of each gene is discussed based on conserved protein domains
994 and homology to other model systems, including lambda, T4, P2, and Mu phages.

995

996 **Acknowledgements**

997 We would like to thank Evelien Adriaenssens for helpful guidance with the taxonomic
998 classification of prophage regions.

999

1000 **Author Contributions**

Contributor Role	Role Definition
Conceptualization	Sarah Bordenstein and Seth Bordenstein
Data Curation	Sarah Bordenstein
Formal Analysis	Sarah Bordenstein and Seth Bordenstein
Funding Acquisition	Seth Bordenstein
Investigation	Sarah Bordenstein
Methodology	Sarah Bordenstein and Seth Bordenstein
Project Administration	Sarah Bordenstein
Resources	Sarah Bordenstein and Seth Bordenstein
Software	Sarah Bordenstein
Supervision	Sarah Bordenstein and Seth Bordenstein
Validation	Sarah Bordenstein and Seth Bordenstein
Visualization	Sarah Bordenstein
Writing – Original Draft Preparation	Sarah Bordenstein
Writing – Review & Editing	Sarah Bordenstein and Seth Bordenstein

1001

1002 **List of Abbreviations**

1003 CI – cytoplasmic incompatibility

1004 EAM – eukaryotic association module

1005 GTA – gene transfer agent

1006 ICTV - International Committee on Taxonomy of Viruses

1007 IS – insertion sequence

1008 HTH – helix-turn-helix

1009 NCBI – National Center for Biotechnology Information

1010 Rpn – recombination-promotion nuclease

1011 RT – reverse transcriptase of group II intron origin

1012 VNTR – variable number tandem repeat

1013 WO-PC1 – WO protein cluster 1

1014 WO-PC2 – WO protein cluster 2

1015 **References**

- 1016 1. Newton IL, Bordenstein SR. Correlations between bacterial ecology and mobile DNA.
1017 *Curr Microbiol.* 2011;62(1):198-208. doi: 10.1007/s00284-010-9693-3. pmid: 20577742
- 1018 2. Cerveau N, Leclercq S, Leroy E, Bouchon D, Cordaux R. Short- and long-term
1019 evolutionary dynamics of bacterial insertion sequences: insights from *Wolbachia*
1020 endosymbionts. *Genome Biol Evol.* 2011;3:1175-86. doi: 10.1093/gbe/evr096. pmid: 21940637
- 1021 3. Masui S, Kamoda S, Sasaki T, Ishikawa H. Distribution and evolution of bacteriophage
1022 WO in *Wolbachia*, the endosymbiont causing sexual alterations in arthropods. *J Mol Evol.*
1023 2000;51(5):491-7. doi: 10.1007/s002390010112. pmid: 11080372
- 1024 4. Kent BN, Bordenstein SR. Phage WO of *Wolbachia*: lambda of the endosymbiont world.
1025 *Trends Microbiol.* 2010;18(4):173-81. doi: 10.1016/j.tim.2009.12.011. pmid: 20083406
- 1026 5. Reveillaud J, Bordenstein SR, Cruaud C, Shaiber A, Esen OC, Weill M, et al. The
1027 *Wolbachia* mobilome in *Culex pipiens* includes a putative plasmid. *Nat Commun.*
1028 2019;10(1):1051. doi: 10.1038/s41467-019-08973-w. pmid: 30837458
- 1029 6. Baiao GC, Janice J, Galinou M, Klasson L. Comparative genomics reveals factors
1030 associated with phenotypic expression of *Wolbachia*. *Genome Biol Evol.* 2021. doi:
1031 10.1093/gbe/evab111. pmid: 34003269
- 1032 7. Kaur R, Shropshire JD, Cross KL, Leigh B, Mansueto AJ, Stewart V, et al. Living in the
1033 endosymbiotic world of *Wolbachia*: A centennial review. *Cell Host Microbe.* 2021;29(6):879-93.
1034 doi: 10.1016/j.chom.2021.03.006. pmid: 33945798
- 1035 8. Weinert LA, Araujo-Jnr EV, Ahmed MZ, Welch JJ. The incidence of bacterial
1036 endosymbionts in terrestrial arthropods. *Proc Biol Sci.* 2015;282(1807):20150249. doi:
1037 doi:10.1098/rspb.2015.0249. pmid: 25904667
- 1038 9. Pruneau L, Moumene A, Meyer DF, Marcelino I, Lefrancois T, Vachiery N. Understanding
1039 *Anaplasmataceae* pathogenesis using "Omics" approaches. *Front Cell Infect Microbiol.*
1040 2014;4:86. doi: 10.3389/fcimb.2014.00086. pmid: 25072029
- 1041 10. Vavre F, Fleury F, Lepetit D, Fouillet P, Bouletreau M. Phylogenetic evidence for
1042 horizontal transmission of *Wolbachia* in host-parasitoid associations. *Mol Biol Evol.*
1043 1999;16(12):1711-23. doi: 10.1093/oxfordjournals.molbev.a026084. pmid: 10605113
- 1044 11. Boyle L, O'Neill SL, Robertson HM, Karr TL. Interspecific and intraspecific horizontal
1045 transfer of *Wolbachia* in *Drosophila*. *Science.* 1993;260(5115):1796-9. doi:
1046 10.1126/science.8511587. pmid: 8511587
- 1047 12. Chafee ME, Funk DJ, Harrison RG, Bordenstein SR. Lateral phage transfer in obligate
1048 intracellular bacteria (*Wolbachia*): verification from natural populations. *Mol Biol Evol.*
1049 2010;27(3):501-5. doi: 10.1093/molbev/msp275. pmid: 19906794
- 1050 13. Wang N, Jia S, Xu H, Liu Y, Huang D. Multiple Horizontal Transfers of Bacteriophage WO
1051 and Host *Wolbachia* in Fig Wasps in a Closed Community. *Front Microbiol.* 2016;7:136. doi:
1052 10.3389/fmicb.2016.00136. pmid: 26913026
- 1053 14. Kent BN, Salichos L, Gibbons JG, Rokas A, Newton IL, Clark ME, et al. Complete
1054 bacteriophage transfer in a bacterial endosymbiont (*Wolbachia*) determined by targeted
1055 genome capture. *Genome Biol Evol.* 2011;3:209-18. doi: 10.1093/gbe/evr007. pmid: 21292630

- 1056 15. Gavotte L, Henri H, Stouthamer R, Charif D, Charlat S, Bouletreau M, et al. A Survey of
1057 the bacteriophage WO in the endosymbiotic bacteria *Wolbachia*. Mol Biol Evol. 2007;24(2):427-
1058 35. doi: 10.1093/molbev/msl171. pmid: 17095536
- 1059 16. Bordenstein SR, Wernegreen JJ. Bacteriophage flux in endosymbionts (*Wolbachia*):
1060 infection frequency, lateral transfer, and recombination rates. Mol Biol Evol. 2004;21(10):1981-
1061 91. doi: 10.1093/molbev/msh211. pmid: 15254259
- 1062 17. Ishmael N, Dunning Hotopp JC, Ioannidis P, Biber S, Sakamoto J, Siozios S, et al.
1063 Extensive genomic diversity of closely related *Wolbachia* strains. Microbiology. 2009;155(Pt
1064 7):2211-22. doi: 10.1099/mic.0.027581-0. pmid: 19389774
- 1065 18. Kent BN, Funkhouser LJ, Setia S, Bordenstein SR. Evolutionary genomics of a temperate
1066 bacteriophage in an obligate intracellular bacteria (*Wolbachia*). PLoS One. 2011;6(9):e24984.
1067 doi: 10.1371/journal.pone.0024984. pmid: 21949820
- 1068 19. Klasson L, Westberg J, Sapountzis P, Naslund K, Lutnaes Y, Darby AC, et al. The mosaic
1069 genome structure of the *Wolbachia* wRi strain infecting *Drosophila simulans*. Proc Natl Acad Sci
1070 U S A. 2009;106(14):5725-30. doi: 10.1073/pnas.0810753106. pmid: 19307581
- 1071 20. Sanogo YO, Dobson SL. WO bacteriophage transcription in *Wolbachia*-infected *Culex*
1072 *pipiens*. Insect Biochem Mol Biol. 2006;36(1):80-5. doi: 10.1016/j.ibmb.2005.11.001. pmid:
1073 16360953
- 1074 21. Werren JH, Baldo L, Clark ME. *Wolbachia*: master manipulators of invertebrate biology.
1075 Nat Rev Microbiol. 2008;6(10):741-51. doi: 10.1038/nrmicro1969. pmid: 18794912
- 1076 22. Charlat S, Hurst GD, Mercot H. Evolutionary consequences of *Wolbachia* infections.
1077 Trends Genet. 2003;19(4):217-23. doi: 10.1016/S0168-9525(03)00024-6. pmid: 12683975
- 1078 23. Fenn K, Blaxter M. *Wolbachia* genomes: revealing the biology of parasitism and
1079 mutualism. Trends Parasitol. 2006;22(2):60-5. doi: 10.1016/j.pt.2005.12.012. pmid: 16406333
- 1080 24. Slatko BE, Taylor MJ, Foster JM. The *Wolbachia* endosymbiont as an anti-filarial
1081 nematode target. Symbiosis. 2010;51(1):55-65. doi: 10.1007/s13199-010-0067-1. pmid:
1082 20730111
- 1083 25. Yamada R, Iturbe-Ormaetxe I, Brownlie JC, O'Neill SL. Functional test of the influence of
1084 *Wolbachia* genes on cytoplasmic incompatibility expression in *Drosophila melanogaster*. Insect
1085 Mol Biol. 2011;20(1):75-85. doi: 10.1111/j.1365-2583.2010.01042.x. pmid: 20854481
- 1086 26. Sinkins SP, Walker T, Lynd AR, Steven AR, Makepeace BL, Godfray HC, et al. *Wolbachia*
1087 variability and host effects on crossing type in *Culex* mosquitoes. Nature. 2005;436(7048):257-
1088 60. doi: 10.1038/nature03629. pmid: 16015330
- 1089 27. Duron O, Fort P, Weill M. Hypervariable prophage WO sequences describe an
1090 unexpected high number of *Wolbachia* variants in the mosquito *Culex pipiens*. Proc Biol Sci.
1091 2006;273(1585):495-502. doi: 10.1098/rspb.2005.3336. pmid: 16615218
- 1092 28. Duron O, Bernard C, Unal S, Berthomieu A, Berticat C, Weill M. Tracking factors
1093 modulating cytoplasmic incompatibilities in the mosquito *Culex pipiens*. Mol Ecol.
1094 2006;15(10):3061-71. doi: 10.1111/j.1365-294X.2006.02996.x. pmid: 16911221
- 1095 29. LePage DP, Metcalf JA, Bordenstein SR, On J, Perlmutter JI, Shropshire JD, et al.
1096 Prophage WO genes recapitulate and enhance *Wolbachia*-induced cytoplasmic incompatibility.
1097 Nature. 2017;543(7644):243-7. doi: 10.1038/nature21391. pmid: 28241146

- 1098 30. Shropshire JD, On J, Layton EM, Zhou H, Bordenstein SR. One prophage WO gene
1099 rescues cytoplasmic incompatibility in *Drosophila melanogaster*. Proc Natl Acad Sci U S A.
1100 2018;115(19):4987-91. doi: 10.1073/pnas.1800650115. pmid: 29686091
- 1101 31. Chen H, Ronau JA, Beckmann JF, Hochstrasser M. A *Wolbachia* nuclease and its binding
1102 partner provide a distinct mechanism for cytoplasmic incompatibility. Proc Natl Acad Sci U S A.
1103 2019;116(44):22314-21. doi: 10.1073/pnas.1914571116. pmid: 31615889
- 1104 32. Beckmann JF, Ronau JA, Hochstrasser M. A *Wolbachia* deubiquitylating enzyme induces
1105 cytoplasmic incompatibility. Nat Microbiol. 2017;2:17007. doi: 10.1038/nmicrobiol.2017.7.
1106 pmid: 28248294
- 1107 33. Perlmutter JI, Bordenstein SR, Unckless RL, LePage DP, Metcalf JA, Hill T, et al. The phage
1108 gene *wmk* is a candidate for male killing by a bacterial endosymbiont. PLoS Pathog.
1109 2019;15(9):e1007936. doi: 10.1371/journal.ppat.1007936. pmid: 31504075
- 1110 34. Bordenstein SR, Marshall ML, Fry AJ, Kim U, Wernegreen JJ. The tripartite associations
1111 between bacteriophage, *Wolbachia*, and arthropods. PLoS Pathog. 2006;2(5):e43. doi:
1112 10.1371/journal.ppat.0020043. pmid: 16710453
- 1113 35. Wright JD, Sjostrand FS, Portaro JK, Barr AR. The ultrastructure of the rickettsia-like
1114 microorganism *Wolbachia pipientis* and associated virus-like bodies in the mosquito *Culex*
1115 *pipiens*. J Ultrastruct Res. 1978;63(1):79-85. doi: 10.1016/s0022-5320(78)80046-x pmid: 671578
- 1116 36. Biliske JA, Batista PD, Grant CL, Harris HL. The bacteriophage WORiC is the active phage
1117 element in *wRi* of *Drosophila simulans* and represents a conserved class of WO phages. BMC
1118 Microbiol. 2011;11:251. doi: 10.1186/1471-2180-11-251. pmid: 22085419
- 1119 37. Fujii Y, Kubo T, Ishikawa H, Sasaki T. Isolation and characterization of the bacteriophage
1120 WO from *Wolbachia*, an arthropod endosymbiont. Biochem Biophys Res Commun.
1121 2004;317(4):1183-8. doi: 10.1016/j.bbrc.2004.03.164. pmid: 15094394
- 1122 38. Tanaka K, Furukawa S, Nikoh N, Sasaki T, Fukatsu T. Complete WO phage sequences
1123 reveal their dynamic evolutionary trajectories and putative functional elements required for
1124 integration into the *Wolbachia* genome. Appl Environ Microbiol. 2009;75(17):5676-86. doi:
1125 10.1128/AEM.01172-09. pmid: 19592535
- 1126 39. Bordenstein SR, Bordenstein SR. Eukaryotic association module in phage WO genomes
1127 from *Wolbachia*. Nat Commun. 2016;7:13155. doi: 10.1038/ncomms13155. pmid: 27727237
- 1128 40. Iturbe-Ormaetxe I, Burke GR, Riegler M, O'Neill SL. Distribution, expression, and motif
1129 variability of ankyrin domain genes in *Wolbachia pipientis*. J Bacteriol. 2005;187(15):5136-45.
1130 doi: 10.1128/JB.187.15.5136-5145.2005. pmid: 16030207
- 1131 41. Siozios S, Ioannidis P, Klasson L, Andersson SG, Braig HR, Bourtzis K. The diversity and
1132 evolution of *Wolbachia* ankyrin repeat domain genes. PLoS One. 2013;8(2):e55390. doi:
1133 10.1371/journal.pone.0055390. pmid: 23390535
- 1134 42. Jahn MT, Arkhipova K, Markert SM, Stigloher C, Lachnit T, Pita L, et al. A Phage Protein
1135 Aids Bacterial Symbionts in Eukaryote Immune Evasion. Cell Host Microbe. 2019;26(4):542-50
1136 e5. doi: 10.1016/j.chom.2019.08.019. pmid: 31561965
- 1137 43. National Library of Medicine (US) National Center for Biotechnology Information.
1138 National Center for Biotechnology Information (NCBI) Bethesda (MD)1988. Available from:
1139 <https://www.ncbi.nlm.nih.gov/>.

- 1140 44. International Committee on Taxonomy of Viruses Executive Committee. The new scope
1141 of virus taxonomy: partitioning the virosphere into 15 hierarchical ranks. *Nat Microbiol.*
1142 2020;5(5):668-74. doi: 10.1038/s41564-020-0709-x. pmid: 32341570
- 1143 45. Simmonds P, Adams MJ, Benko M, Breitbart M, Brister JR, Carstens EB, et al. Consensus
1144 statement: Virus taxonomy in the age of metagenomics. *Nat Rev Microbiol.* 2017;15(3):161-8.
1145 doi: 10.1038/nrmicro.2016.177. pmid: 28134265
- 1146 46. Lindsey ARI, Rice DW, Bordenstein SR, Brooks AW, Bordenstein SR, Newton ILG.
1147 Evolutionary Genetics of Cytoplasmic Incompatibility Genes *cifA* and *cifB* in Prophage WO of
1148 *Wolbachia*. *Genome Biol Evol.* 2018;10(2):434-51. doi: 10.1093/gbe/evy012. pmid: 29351633
- 1149 47. Martinez J, Klasson L, Welch JJ, Jiggins FM. Life and Death of Selfish Genes: Comparative
1150 Genomics Reveals the Dynamic Evolution of Cytoplasmic Incompatibility. *Mol Biol Evol.*
1151 2021;38(1):2-15. doi: 10.1093/molbev/msaa209. pmid: 32797213
- 1152 48. Wu M, Sun LV, Vamathevan J, Riegler M, Deboy R, Brownlie JC, et al. Phylogenomics of
1153 the reproductive parasite *Wolbachia pipientis* wMel: a streamlined genome overrun by mobile
1154 genetic elements. *PLoS Biol.* 2004;2(3):E69. doi: 10.1371/journal.pbio.0020069. pmid:
1155 15024419
- 1156 49. Crainey JL, Hurst J, Lamberton PHL, Cheke RA, Griffin CE, Wilson MD, et al. The Genomic
1157 Architecture of Novel *Simulium damnosum* *Wolbachia* Prophage Sequence Elements and
1158 Implications for Onchocerciasis Epidemiology. *Front Microbiol.* 2017;8:852. doi:
1159 10.3389/fmicb.2017.00852. pmid: 28611731
- 1160 50. Smith MCM. Phage-encoded Serine Integrases and Other Large Serine Recombinases.
1161 *Microbiol Spectr.* 2015;3(4). doi: 10.1128/microbiolspec.MDNA3-0059-2014. pmid: 26350324
- 1162 51. Metcalf JA, Jo M, Bordenstein SR, Jaenike J, Bordenstein SR. Recent genome reduction
1163 of *Wolbachia* in *Drosophila recens* targets phage WO and narrows candidates for reproductive
1164 parasitism. *PeerJ.* 2014;2:e529. doi: 10.7717/peerj.529. pmid: 25165636
- 1165 52. Newton IL, Clark ME, Kent BN, Bordenstein SR, Qu J, Richards S, et al. Comparative
1166 Genomics of Two Closely Related *Wolbachia* with Different Reproductive Effects on Hosts.
1167 *Genome Biol Evol.* 2016;8(5):1526-42. doi: 10.1093/gbe/evw096. pmid: 27189996
- 1168 53. Riegler M, Iturbe-Ormaetxe I, Woolfit M, Miller WJ, O'Neill SL. Tandem repeat markers
1169 as novel diagnostic tools for high resolution fingerprinting of *Wolbachia*. *BMC Microbiol.*
1170 2012;12 Suppl 1:S12. doi: 10.1186/1471-2180-12-S1-S12. pmid: 22375862
- 1171 54. Duplouy A, Iturbe-Ormaetxe I, Beatson SA, Szubert JM, Brownlie JC, McMeniman CJ, et
1172 al. Draft genome sequence of the male-killing *Wolbachia* strain wBol1 reveals recent horizontal
1173 gene transfers from diverse sources. *BMC Genomics.* 2013;14:20. doi: 10.1186/1471-2164-14-
1174 20. pmid: 23324387
- 1175 55. Harshey RM. Transposable Phage Mu. *Microbiol Spectr.* 2014;2(5). doi:
1176 10.1128/microbiolspec.MDNA3-0007-2014. pmid: 26104374
- 1177 56. Kampfraath AA, Klasson L, Anvar SY, Vossen R, Roelofs D, Kraaijeveld K, et al. Genome
1178 expansion of an obligate parthenogenesis-associated *Wolbachia* poses an exception to the
1179 symbiont reduction model. *BMC Genomics.* 2019;20(1):106. doi: 10.1186/s12864-019-5492-9.
1180 pmid: 30727958
- 1181 57. Bobay LM, Touchon M, Rocha EP. Pervasive domestication of defective prophages by
1182 bacteria. *Proc Natl Acad Sci U S A.* 2014;111(33):12127-32. doi: 10.1073/pnas.1405336111.
1183 pmid: 25092302

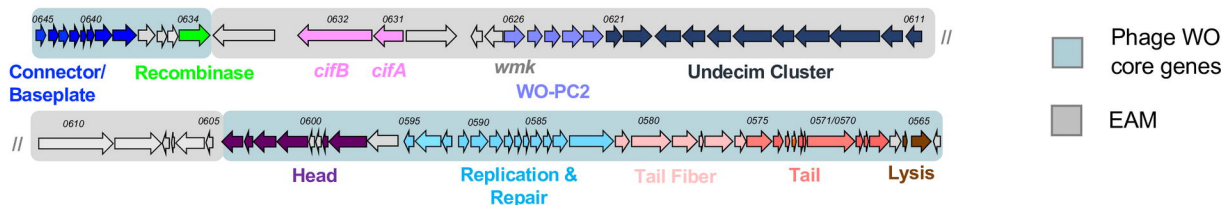
- 1184 58. Ramisetty BCM, Sudhakari PA. Bacterial 'Grounded' Prophages: Hotspots for Genetic
1185 Renovation and Innovation. *Front Genet.* 2019;10:65. doi: 10.3389/fgene.2019.00065. pmid:
1186 30809245
- 1187 59. Fillol-Salom A, Martinez-Rubio R, Abdulrahman RF, Chen J, Davies R, Penades JR. Phage-
1188 inducible chromosomal islands are ubiquitous within the bacterial universe. *ISME J.*
1189 2018;12(9):2114-28. doi: 10.1038/s41396-018-0156-3. pmid: 29875435
- 1190 60. Penades JR, Christie GE. The Phage-Inducible Chromosomal Islands: A Family of Highly
1191 Evolved Molecular Parasites. *Annu Rev Virol.* 2015;2(1):181-201. doi: 10.1146/annurev-
1192 virology-031413-085446. pmid: 26958912
- 1193 61. Ioannidis P, Dunning Hotopp JC, Sapountzis P, Siozios S, Tsiamis G, Bordenstein SR, et al.
1194 New criteria for selecting the origin of DNA replication in *Wolbachia* and closely related
1195 bacteria. *BMC Genomics.* 2007;8:182. doi: 10.1186/1471-2164-8-182. pmid: 17584494
- 1196 62. Rands CM, Brussow H, Zdobnov EM. Comparative genomics groups phages of
1197 *Negativicutes* and classical *Firmicutes* despite different Gram-staining properties. *Environ*
1198 *Microbiol.* 2019;21(11):3989-4001. doi: 10.1111/1462-2920.14746. pmid: 31314945
- 1199 63. Oliveira PH, Touchon M, Cury J, Rocha EPC. The chromosomal organization of horizontal
1200 gene transfer in bacteria. *Nat Commun.* 2017;8(1):841. doi: 10.1038/s41467-017-00808-w.
1201 pmid: 29018197
- 1202 64. Canchaya C, Fournous G, Brussow H. The impact of prophages on bacterial
1203 chromosomes. *Mol Microbiol.* 2004;53(1):9-18. doi: 10.1111/j.1365-2958.2004.04113.x. pmid:
1204 15225299
- 1205 65. Bobay LM, Rocha EP, Touchon M. The adaptation of temperate bacteriophages to their
1206 host genomes. *Mol Biol Evol.* 2013;30(4):737-51. doi: 10.1093/molbev/mss279. pmid:
1207 23243039
- 1208 66. Woolfit M, Iturbe-Ormaetxe I, Brownlie JC, Walker T, Riegler M, Seleznev A, et al.
1209 Genomic evolution of the pathogenic *Wolbachia* strain, *wMelPop*. *Genome Biol Evol.*
1210 2013;5(11):2189-204. doi: 10.1093/gbe/evt169. pmid: 24190075
- 1211 67. Duarte EH, Carvalho A, Lopez-Madrugal S, Costa J, Teixeira L. Forward genetics in
1212 *Wolbachia*: Regulation of *Wolbachia* proliferation by the amplification and deletion of an
1213 addictive genomic island. *PLoS Genet.* 2021;17(6):e1009612. doi:
1214 10.1371/journal.pgen.1009612. pmid: 34143770
- 1215 68. Rohrscheib CE, Frentiu FD, Horn E, Ritchie FK, van Swinderen B, Weible MW, 2nd, et al.
1216 Intensity of Mutualism Breakdown Is Determined by Temperature Not Amplification of
1217 *Wolbachia* Genes. *PLoS Pathog.* 2016;12(9):e1005888. doi: 10.1371/journal.ppat.1005888.
1218 pmid: 27661080
- 1219 69. Chrostek E, Teixeira L. Mutualism breakdown by amplification of *Wolbachia* genes. *PLoS*
1220 *Biol.* 2015;13(2):e1002065. doi: 10.1371/journal.pbio.1002065. pmid: 25668031
- 1221 70. Fallon AM. DNA recombination and repair in *Wolbachia*: RecA and related proteins. *Mol*
1222 *Genet Genomics.* 2021;296(2):437-56. doi: 10.1007/s00438-020-01760-z. pmid: 33507381
- 1223 71. Klasson L, Kambris Z, Cook PE, Walker T, Sinkins SP. Horizontal gene transfer between
1224 *Wolbachia* and the mosquito *Aedes aegypti*. *BMC Genomics.* 2009;10:33. doi: 10.1186/1471-
1225 2164-10-33. pmid: 19154594
- 1226 72. Chrostek E, Marialva MS, Esteves SS, Weinert LA, Martinez J, Jiggins FM, et al. *Wolbachia*
1227 variants induce differential protection to viruses in *Drosophila melanogaster*: a phenotypic and

- 1228 phylogenomic analysis. PLoS Genet. 2013;9(12):e1003896. doi: 10.1371/journal.pgen.1003896.
1229 pmid: 24348259
- 1230 73. Matsuura M, Saldanha R, Ma H, Wank H, Yang J, Mohr G, et al. A bacterial group II
1231 intron encoding reverse transcriptase, maturase, and DNA endonuclease activities: biochemical
1232 demonstration of maturase activity and insertion of new genetic information within the intron.
1233 Genes Dev. 1997;11(21):2910-24. doi: 10.1101/gad.11.21.2910. pmid: 9353259
- 1234 74. Dong X, Qu G, Piazza CL, Belfort M. Group II intron as cold sensor for self-preservation
1235 and bacterial conjugation. Nucleic Acids Res. 2020;48(11):6198-209. doi: 10.1093/nar/gkaa313.
1236 pmid: 32379323
- 1237 75. Baldrige GD, Markowski TW, Witthuhn BA, Higgins L, Baldrige AS, Fallon AM. The
1238 *Wolbachia* WO bacteriophage proteome in the *Aedes albopictus* C/wStr1 cell line: evidence for
1239 lytic activity? In Vitro Cell Dev Biol Anim. 2016;52(1):77-88. doi: 10.1007/s11626-015-9949-0.
1240 pmid: 26427709
- 1241 76. Gillespie JJ, Joardar V, Williams KP, Driscoll T, Hostetler JB, Nordberg E, et al. A *Rickettsia*
1242 genome overrun by mobile genetic elements provides insight into the acquisition of genes
1243 characteristic of an obligate intracellular lifestyle. J Bacteriol. 2012;194(2):376-94. doi:
1244 10.1128/JB.06244-11. pmid: 22056929
- 1245 77. Gutzwiller F, Carmo CR, Miller DE, Rice DW, Newton IL, Hawley RS, et al. Dynamics of
1246 *Wolbachia pipientis* Gene Expression Across the *Drosophila melanogaster* Life Cycle. G3
1247 (Bethesda). 2015;5(12):2843-56. doi: 10.1534/g3.115.021931. pmid: 26497146
- 1248 78. Masui S, Kuroiwa H, Sasaki T, Inui M, Kuroiwa T, Ishikawa H. Bacteriophage WO and
1249 virus-like particles in *Wolbachia*, an endosymbiont of arthropods. Biochem Biophys Res
1250 Commun. 2001;283(5):1099-104. doi: 10.1006/bbrc.2001.4906. pmid: 11355885
- 1251 79. Young R. Bacteriophage lysis: mechanism and regulation. Microbiol Rev. 1992;56(3):430-
1252 81. pmid: 1406491
- 1253 80. Otten C, Brill M, Vollmer W, Viollier PH, Salje J. Peptidoglycan in obligate intracellular
1254 bacteria. Mol Microbiol. 2018;107(2):142-63. doi: 10.1111/mmi.13880. pmid: 29178391
- 1255 81. Bordenstein SR, Bordenstein SR. Temperature affects the tripartite interactions between
1256 bacteriophage WO, *Wolbachia*, and cytoplasmic incompatibility. PLoS One. 2011;6(12):e29106.
1257 doi: 10.1371/journal.pone.0029106. pmid: 22194999
- 1258 82. Rahman MS, Ammerman NC, Sears KT, Ceraul SM, Azad AF. Functional characterization
1259 of a phospholipase A(2) homolog from *Rickettsia typhi*. J Bacteriol. 2010;192(13):3294-303. doi:
1260 10.1128/JB.00155-10. pmid: 20435729
- 1261 83. Sato H, Frank DW. ExoU is a potent intracellular phospholipase. Mol Microbiol.
1262 2004;53(5):1279-90. doi: 10.1111/j.1365-2958.2004.04194.x. pmid: 15387809
- 1263 84. Banerji S, Fliieger A. Patatin-like proteins: a new family of lipolytic enzymes present in
1264 bacteria? Microbiology. 2004;150(Pt 3):522-5. doi: 10.1099/mic.0.26957-0. pmid: 14993300
- 1265 85. Kamilla S, Jain V. Mycobacteriophage D29 holin C-terminal region functionally assists in
1266 holin aggregation and bacterial cell death. FEBS J. 2016;283(1):173-90. doi:
1267 10.1111/febs.13565. pmid: 26471254
- 1268 86. Wang IN, Smith DL, Young R. Holins: the protein clocks of bacteriophage infections.
1269 Annu Rev Microbiol. 2000;54:799-825. doi: 10.1146/annurev.micro.54.1.799. pmid: 11018145

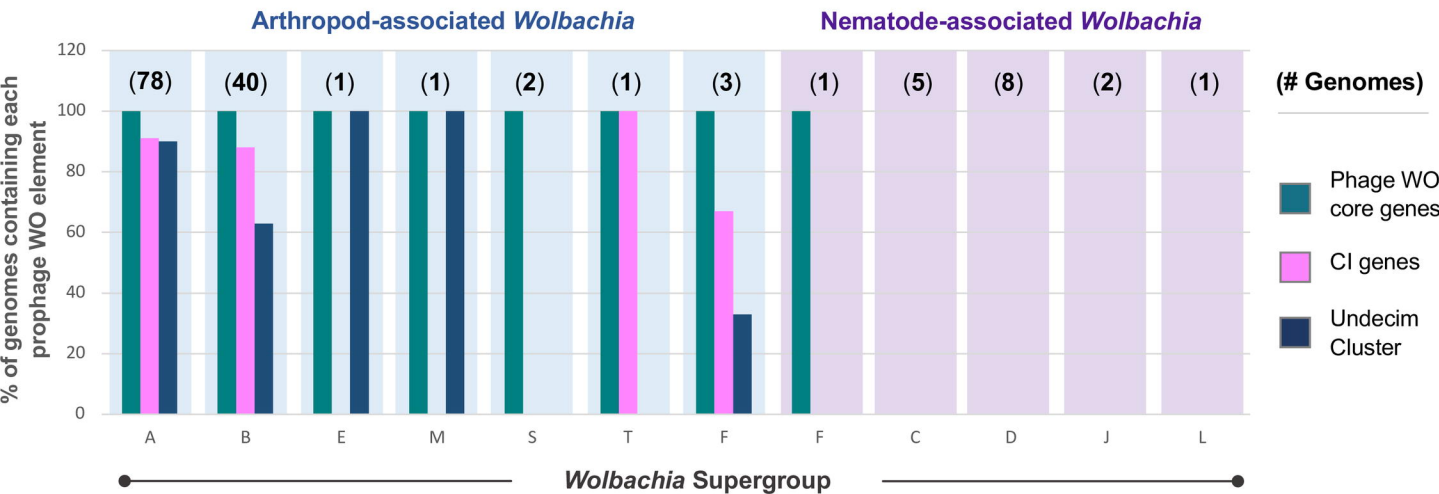
- 1270 87. Lang AS, Beatty JT. Genetic analysis of a bacterial genetic exchange element: the gene
1271 transfer agent of *Rhodobacter capsulatus*. Proc Natl Acad Sci U S A. 2000;97(2):859-64. doi:
1272 10.1073/pnas.97.2.859 pmid: 10639170
- 1273 88. Westbye AB, Beatty JT, Lang AS. Guaranteeing a captive audience: coordinated
1274 regulation of gene transfer agent (GTA) production and recipient capability by cellular
1275 regulators. Curr Opin Microbiol. 2017;38:122-9. doi: 10.1016/j.mib.2017.05.003. pmid:
1276 28599143
- 1277 89. Lang AS, Beatty JT. Importance of widespread gene transfer agent genes in alpha-
1278 proteobacteria. Trends Microbiol. 2007;15(2):54-62. doi: 10.1016/j.tim.2006.12.001. pmid:
1279 17184993
- 1280 90. Dohra H, Tanaka K, Suzuki T, Fujishima M, Suzuki H. Draft genome sequences of three
1281 *Holospira* species (*Holospira obtusa*, *Holospira undulata*, and *Holospira elegans*),
1282 endonuclear symbiotic bacteria of the ciliate *Paramecium caudatum*. FEMS Microbiol Lett.
1283 2014;359(1):16-8. doi: 10.1111/1574-6968.12577. pmid: 25115770
- 1284 91. Kantor RS, Miller SE, Nelson KL. The Water Microbiome Through a Pilot Scale Advanced
1285 Treatment Facility for Direct Potable Reuse. Front Microbiol. 2019;10:993. doi:
1286 10.3389/fmicb.2019.00993. pmid: 31139160
- 1287 92. Tully BJ, Graham ED, Heidelberg JF. The reconstruction of 2,631 draft metagenome-
1288 assembled genomes from the global oceans. Sci Data. 2018;5:170203. doi:
1289 10.1038/sdata.2017.203. pmid: 29337314
- 1290 93. Egan S, Gardiner M. Microbial Dysbiosis: Rethinking Disease in Marine Ecosystems. Front
1291 Microbiol. 2016;7:991. doi: 10.3389/fmicb.2016.00991. pmid: 27446031
- 1292 94. Takano SI, Gotoh Y, Hayashi T. "*Candidatus Mesenet longicola*": Novel Endosymbionts of
1293 *Brontispa longissima* that Induce Cytoplasmic Incompatibility. Microb Ecol. 2021. doi:
1294 10.1007/s00248-021-01686-y. pmid: 33454808
- 1295 95. Rocchi I, Ericson CF, Malter KE, Zargar S, Eisenstein F, Pilhofer M, et al. A Bacterial Phage
1296 Tail-like Structure Kills Eukaryotic Cells by Injecting a Nuclease Effector. Cell Rep.
1297 2019;28(2):295-301 e4. doi: 10.1016/j.celrep.2019.06.019. pmid: 31291567
- 1298 96. Gillespie JJ, Driscoll TP, Verhoeve VI, Rahman MS, Macaluso KR, Azad AF. A Tangled
1299 Web: Origins of Reproductive Parasitism. Genome Biol Evol. 2018;10(9):2292-309. doi:
1300 10.1093/gbe/evy159. pmid: 30060072
- 1301 97. Garushyants SK, Beliavskaia AY, Malko DB, Logacheva MD, Rautian MS, Gelfand MS.
1302 Comparative Genomic Analysis of *Holospira* spp., Intranuclear Symbionts of Paramecia. Front
1303 Microbiol. 2018;9:738. doi: 10.3389/fmicb.2018.00738. pmid: 29713316
- 1304 98. Zdobnov EM, Apweiler R. InterProScan--an integration platform for the signature-
1305 recognition methods in InterPro. Bioinformatics. 2001;17(9):847-8. doi:
1306 10.1093/bioinformatics/17.9.847. pmid: 11590104
- 1307 99. Altschul SF, Gish W, Miller W, Myers EW, Lipman DJ. Basic local alignment search tool. J
1308 Mol Biol. 1990;215(3):403-10. doi: 10.1016/S0022-2836(05)80360-2. pmid: 2231712
- 1309 100. Finn RD, Bateman A, Clements J, Coggill P, Eberhardt RY, Eddy SR, et al. Pfam: the
1310 protein families database. Nucleic Acids Res. 2014;42(Database issue):D222-30. doi:
1311 10.1093/nar/gkt1223. pmid: 24288371

- 1312 101. Soding J, Biegert A, Lupas AN. The HHpred interactive server for protein homology
1313 detection and structure prediction. *Nucleic Acids Res.* 2005;33(Web Server issue):W244-8. doi:
1314 10.1093/nar/gki408. pmid: 15980461
- 1315 102. Siguier P, Perochon J, Lestrade L, Mahillon J, Chandler M. ISfinder: the reference centre
1316 for bacterial insertion sequences. *Nucleic Acids Res.* 2006;34(Database issue):D32-6. doi:
1317 10.1093/nar/gkj014. pmid: 16381877
- 1318 103. Schultz J, Copley RR, Doerks T, Ponting CP, Bork P. SMART: a web-based tool for the
1319 study of genetically mobile domains. *Nucleic Acids Res.* 2000;28(1):231-4. doi:
1320 10.1093/nar/28.1.231. pmid: 10592234
- 1321 104. Darling AC, Mau B, Blattner FR, Perna NT. Mauve: multiple alignment of conserved
1322 genomic sequence with rearrangements. *Genome Res.* 2004;14(7):1394-403. doi:
1323 10.1101/gr.2289704. pmid: 15231754
- 1324 105. Edgar RC. MUSCLE: multiple sequence alignment with high accuracy and high
1325 throughput. *Nucleic Acids Res.* 2004;32(5):1792-7. doi: 10.1093/nar/gkh340. pmid: 15034147
- 1326 106. Darriba D, Taboada GL, Doallo R, Posada D. ProtTest 3: fast selection of best-fit models
1327 of protein evolution. *Bioinformatics.* 2011;27(8):1164-5. doi: 10.1093/bioinformatics/btr088.
1328 pmid: 21335321
- 1329 107. Guindon S, Gascuel O. A simple, fast, and accurate algorithm to estimate large
1330 phylogenies by maximum likelihood. *Syst Biol.* 2003;52(5):696-704. doi:
1331 10.1080/10635150390235520. pmid: 14530136
- 1332 108. Ronquist F, Teslenko M, van der Mark P, Ayres DL, Darling A, Höhna S, et al. MrBayes
1333 3.2: efficient Bayesian phylogenetic inference and model choice across a large model space.
1334 *Syst Biol.* 2012;61(3):539-42. doi: 10.1093/sysbio/sys029. pmid: 22357727
- 1335 109. Turner D, Kropinski AM, Adriaenssens EM. A Roadmap for Genome-Based Phage
1336 Taxonomy. *Viruses.* 2021;13(3):506. doi: 10.3390/v13030506 pmid: doi:10.3390/v13030506
- 1337 110. Klasson L, Walker T, Sebahia M, Sanders MJ, Quail MA, Lord A, et al. Genome evolution
1338 of *Wolbachia* strain wPip from the *Culex pipiens* group. *Mol Biol Evol.* 2008;25(9):1877-87. doi:
1339 10.1093/molbev/msn133. pmid: 18550617
- 1340

a Genomic map of prophage WOMeIB

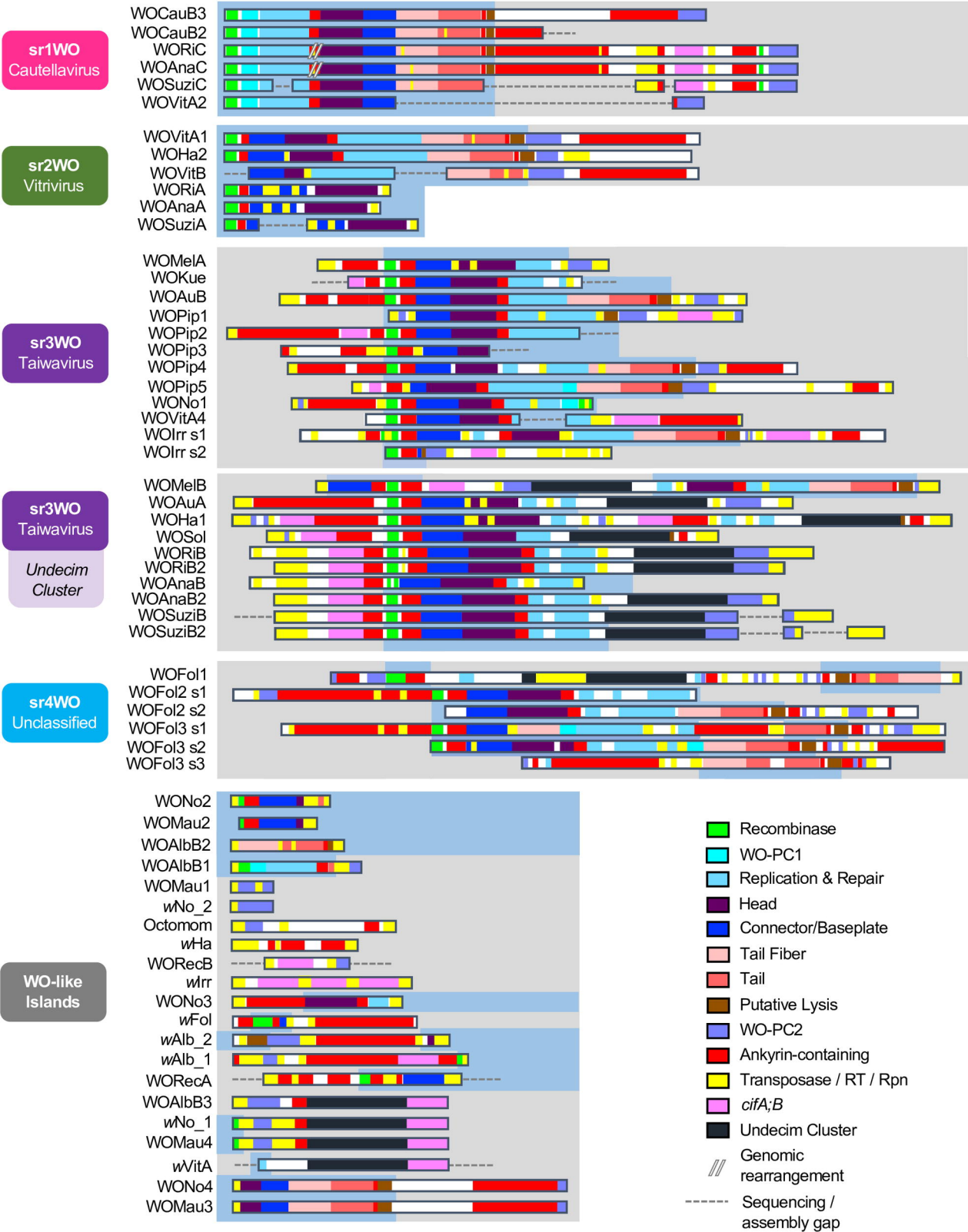


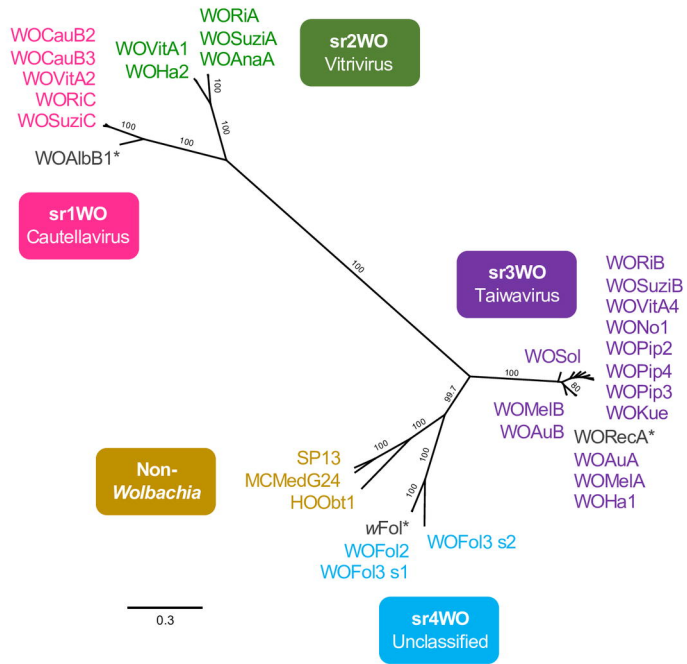
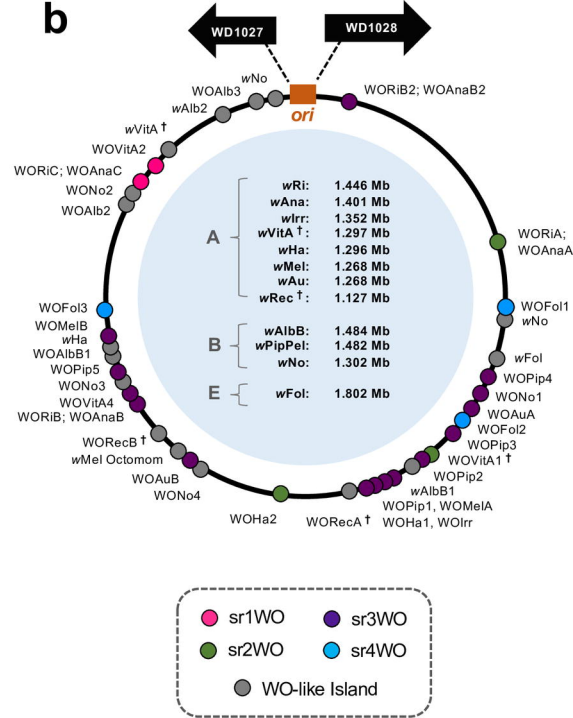
b Prophage WO elements across *Wolbachia* supergroups

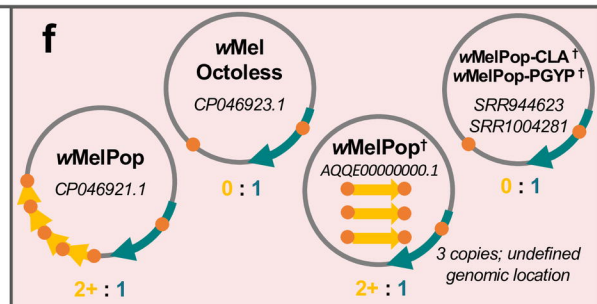
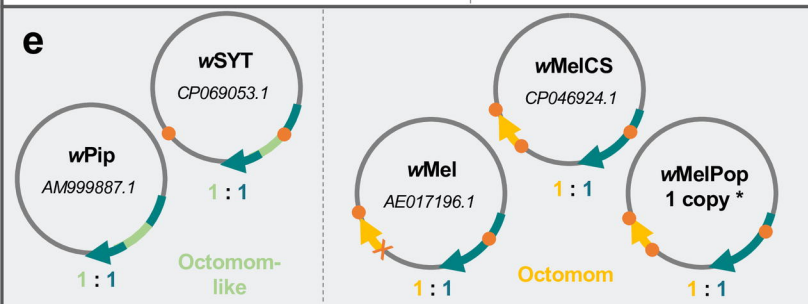
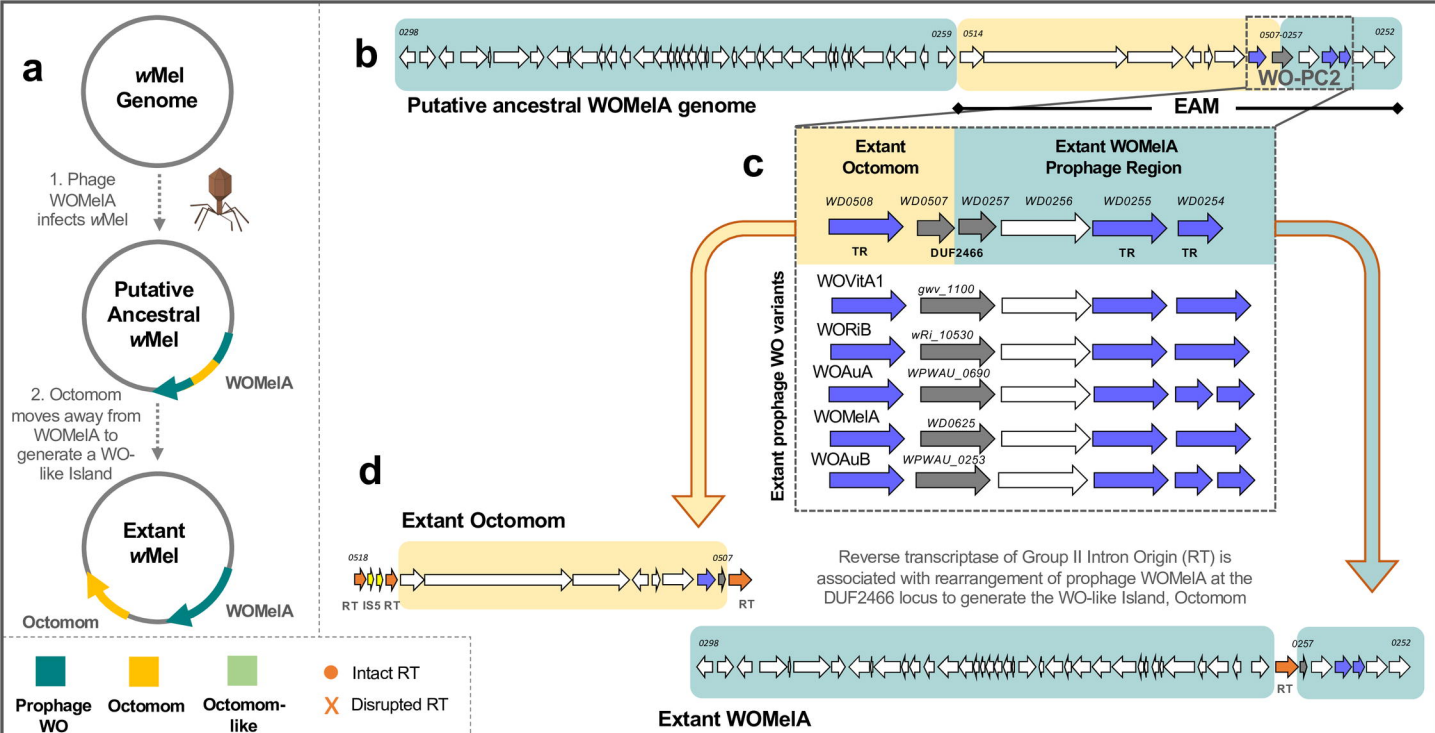


Core Prophage WO

Eukaryotic Association Module



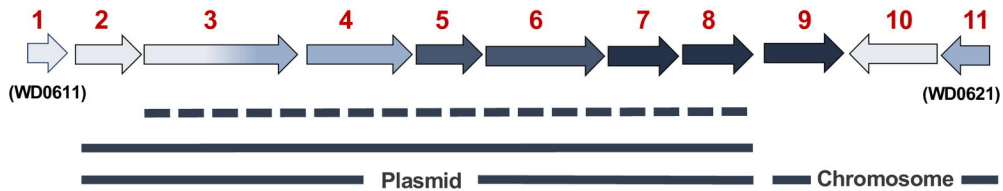
a**b**



Normal *Wolbachia* proliferation; Non-pathogenic

Over-proliferation of *Wolbachia*; Pathogenic

a Undecim Cluster



WOMeIB

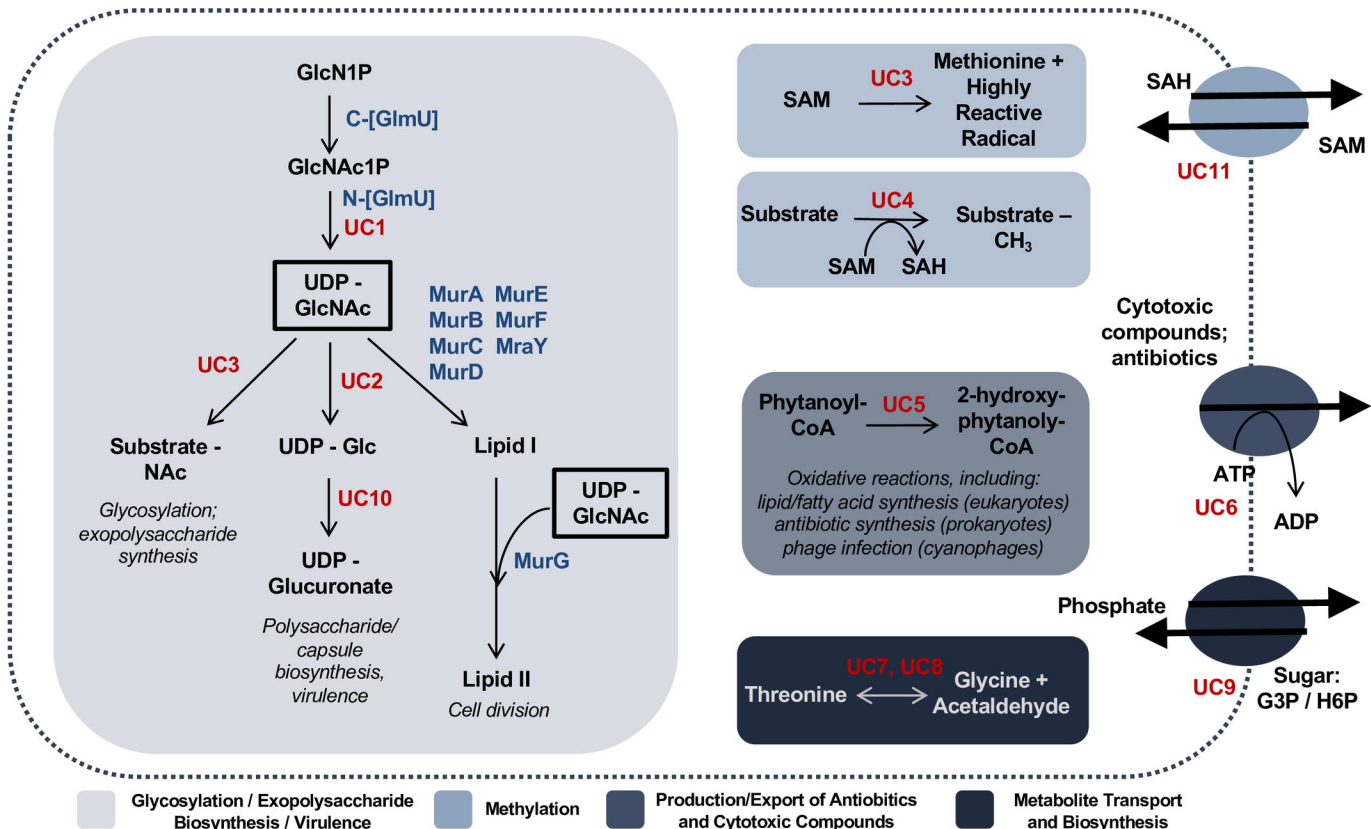
Cardinium hertigii cHgTN10 (67%)

Phycorickettsia trachydisci (68%)

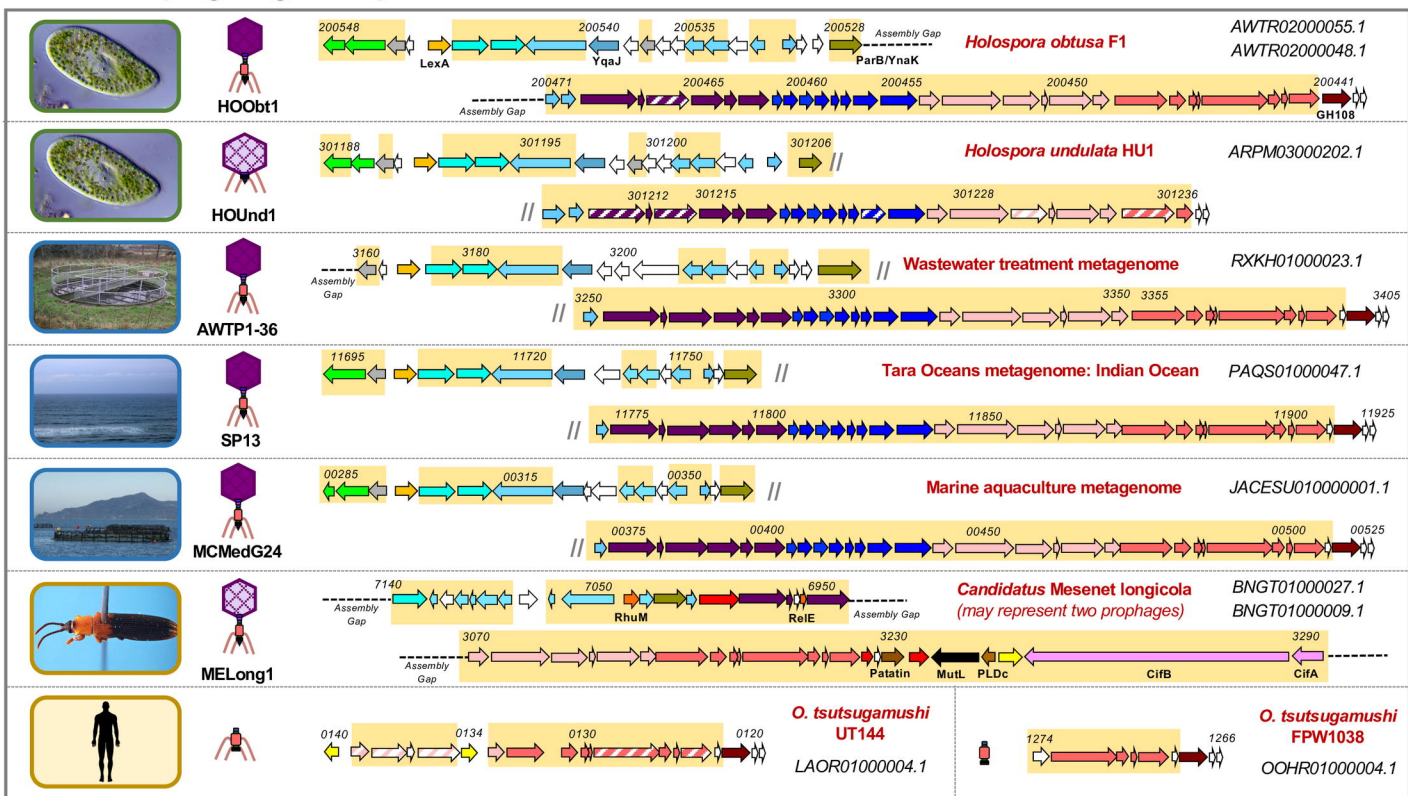
Rickettsia sp. (p: 74%) (c: 67%)

Nucleotide
Identity

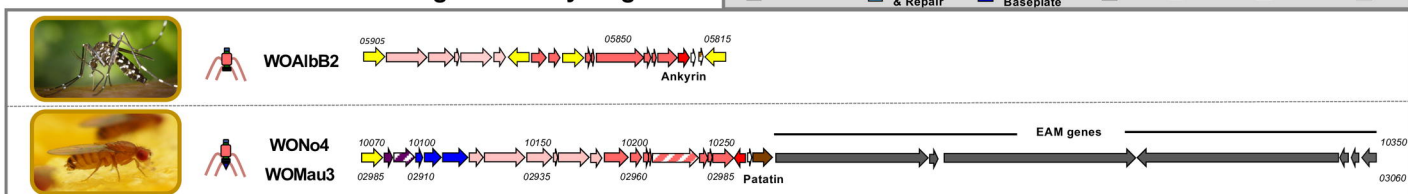
b

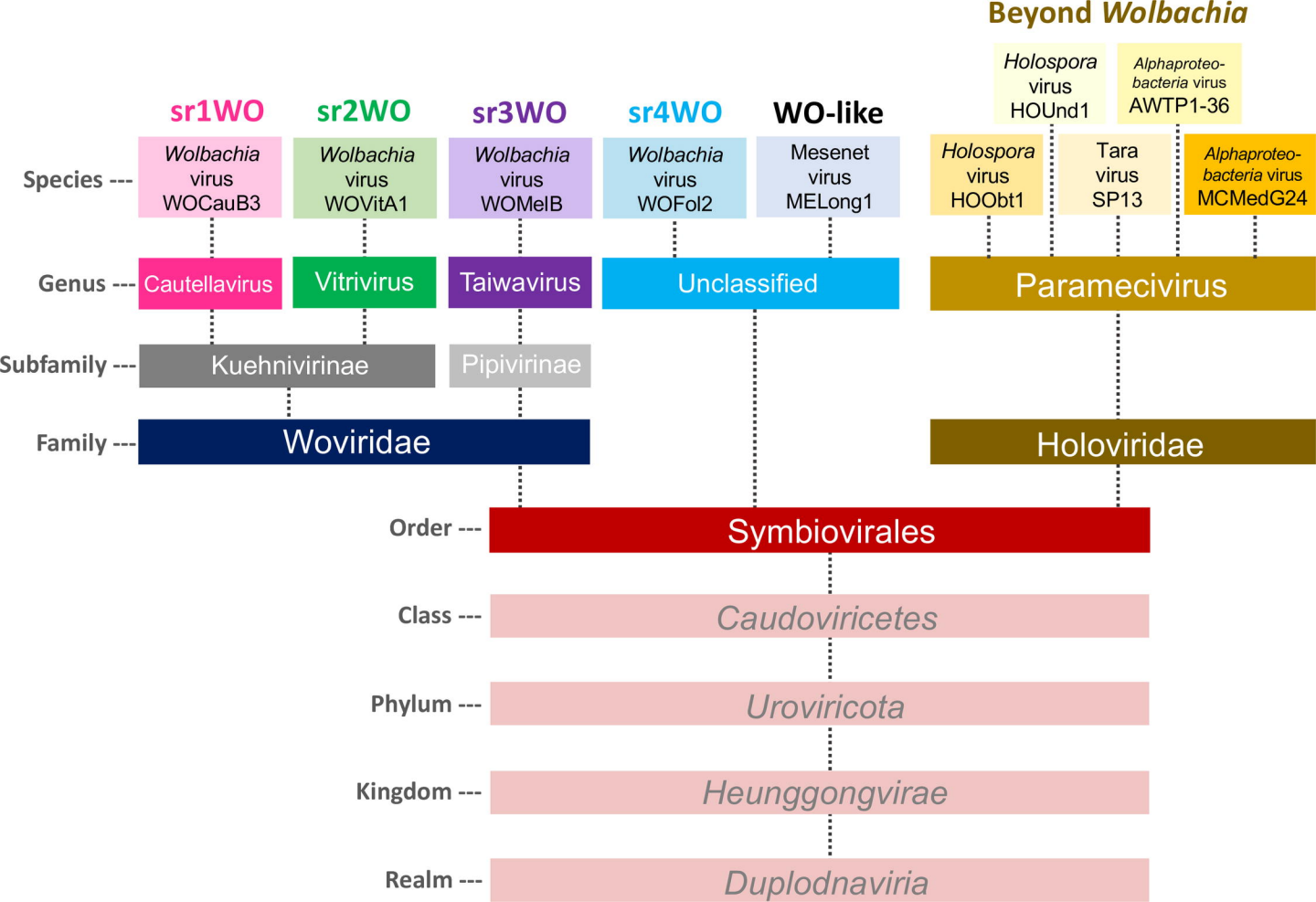


a Wo-like Prophage Regions Beyond Wolbachia



b Wolbachia WO-like Islands featuring Tail and Lysis genes





a	Distinguishing Order Traits	Symbiovirales			
	Host: symbiotic bacteria	✓	✓	✓	✓
	Core phage modules: recombinase, replication, head, connector/baseplate, tail fiber, contractile tail, lysis	✓	✓	✓	✓
	Large serine recombinase (typing gene) PAAR gene in connector/baseplate module	✓	✓	✓	✓

b	Distinguishing Family Traits	Woviridae	Holoviridae
	EAM	✓	Absent
	Ankyrin-repeat containing proteins	✓	Absent
	HTH_XRE transcriptional regulators	✓	Absent
Putative lysis gene	Patatin	GH108	

c	Distinguishing Subfamily Traits	Kuehnavirinae	Pipivirinae
	Integrate into distinct <i>att</i> sites	✓	----
	Location of EAM in prophage genome	3'-prophage genome	Flanking one or both sides

d	Distinguishing Genus Traits	Cautellavirus	Vitrovirus	Taiwavirus	Paramecivirus
	Chromosomal integration	Magnesium chelatase gene or Sua5-intergenic region	VNTR-105	Flanked by EAM, mobile elements	Unknown
	Structural module synteny: baseplate -> head -> replication & repair -> tail	✓	----	----	✓
	Structural module synteny: replication & repair -> head -> baseplate -> tail	----	✓	✓	----
	Direction of ankyrin adjacent to late control gene (relative to tail/patatin)	Opposite	Same	Same	N/A
	WO-PC1	✓	Absent	Some	✓
	ParB	Absent	✓	✓	✓
	Transcriptional regulators (HTH_XRE)	1-domain	2-domain	2-domain	Absent
	Undecim Cluster	Absent	Absent	Some	Absent
	CifA;B	Some	Absent	Some	Absent
	MutL	Absent	✓	Some	Absent